

## **General Disclaimer**

### **One or more of the Following Statements may affect this Document**

- This document has been reproduced from the best copy furnished by the organizational source. It is being released in the interest of making available as much information as possible.
- This document may contain data, which exceeds the sheet parameters. It was furnished in this condition by the organizational source and is the best copy available.
- This document may contain tone-on-tone or color graphs, charts and/or pictures, which have been reproduced in black and white.
- This document is paginated as submitted by the original source.
- Portions of this document are not fully legible due to the historical nature of some of the material. However, it is the best reproduction available from the original submission.

**NASA TECHNICAL  
MEMORANDUM**

**NASA TM X-62,491**

**NASA TM X-62,491**

(NASA-TM-X-62491) COMPARISON OF MODEL AND  
FLIGHT TEST DATA FOR AN AUGMENTED JET FLAP  
STOL RESEARCH AIRCRAFT (NASA) 45 p HC \$3.75  
CSCL 01C

**N76-10093**

**G3/05    Unclass  
39437**

**COMPARISON OF MODEL AND FLIGHT TEST DATA FOR AN  
AUGMENTED JET FLAP STOL RESEARCH AIRCRAFT**

**W. L. Cook and D. C. Whittley**

**Ames Research Center  
Moffett Field, Calif. 94035**

**and**

**de Havilland Aircraft of Canada Ltd.  
Downsview, Ontario, Canada**

**June 1975**



1. Report No. TM X-62,491	2. Government Accession No.	3. Recipient's Catalog No.	
4. Title and Subtitle COMPARISON OF MODEL AND FLIGHT TEST DATA FOR AN AUGMENTED JET FLAP STOL RESEARCH AIRCRAFT		5. Report Date	
		6. Performing Organization Code	
7. Author(s) W. L. Cook and D. C. Whittley		8. Performing Organization Report No. A-6303	
		10. Work Unit No. 514-50-01-01	
9. Performing Organization Name and Address NASA Ames Research Center Moffett Field, Calif. 94035 and de Havilland Aircraft of Canada Ltd. Downsview, Ontario, Canada		11. Contract or Grant No.	
		13. Type of Report and Period Covered Technical Memorandum	
12. Sponsoring Agency Name and Address National Aeronautics and Space Administration Washington, D. C. 20546		14. Sponsoring Agency Code	
		15. Supplementary Notes	
16. Abstract <p>Aerodynamic design data for the Augmented Jet Flap STOL Research Aircraft or commonly known as the Augmentor-Wing Jet-STOL Research Aircraft was based on results of tests carried out on a large scale research model in the NASA Ames 40- by 80-Foot Wind Tunnel. Since the model differs in some respects from the aircraft, precise correlation between tunnel and flight test is not expected, however the paper delineates the major areas of confidence derived from the wind tunnel tests and shows that, for the most part, tunnel results compare favourably with flight experience. In some areas the model tests were known to be non-representative so that a degree of uncertainty remained: these areas of greater uncertainty are identified and again discussed in the light subsequent flight tests.</p>			
17. Key Words (Suggested by Author(s)) STOL Augmented jet flap Aerodynamics		18. Distribution Statement Unlimited  STAR Category - 02,05, 07,08	
19. Security Classif. (of this report) Unclassified	20. Security Classif. (of this page) Unclassified	21. No. of Pages 44	22. Price* \$3.75

## NOTATION

A	augmentation ratio
$C_D$	drag coefficient, $\frac{\text{drag}}{qs}$
$C_j$	blowing momentum coefficient, $\frac{X_B}{qs}$
$C_L$	lift coefficient, $\frac{\text{lift}}{qs}$
$C_\ell$	rolling moment coefficient
$C_T$	thrust coefficient vectored hot thrust $\frac{X_V}{qs}$
$N_H$	engine high speed
V	velocity
$X_B$	engine fan air blowing thrust
$X_V$	engine vectored hot thrust
c	wing chord length
h	height above ground
q	free stream dynamic pressure
$\alpha$	wing angle of attack
$\rho$	mass density of ambient air
$\delta_A$	aileron deflection
$\delta_F$	trailing edge flap deflection angle
$\delta_e$	elevator deflection angle
$\delta_{TH}$	vectored hot thrust nozzle deflection angle
$\delta_w$	control wheel angle
$\eta$	nozzle efficiency
$\phi$	roll angle
$\ddot{\phi}$	roll acceleration, rad/sec <sup>2</sup>

### Subscripts

- A free air or aileron
- $\beta$  sideslip angle
- F trailing edge flaps
- I isentropic
- G in ground effect

COMPARISON OF MODEL AND FLIGHT TEST DATA FOR AN AUGMENTED

JET FLAP STOL RESEARCH AIRCRAFT

by

W. L. Cook  
Chief, Research Aircraft Projects Office  
NASA, Ames Research Center  
Moffett Field, California 94035

and

D. C. Whittley  
Manager, Research & Augmentor Technology  
De Havilland Aircraft of Canada Limited,  
Downsview, Ontario, Canada

SUMMARY

Aerodynamic design data for the Augmented Jet Flap STOL Research Aircraft or commonly known as the Augmentor-Wing Jet-STOL Research Aircraft was based on results of tests carried out on a large scale research model in the NASA Ames 40- by 80-Foot Wind Tunnel. Since the model differs in some respects from the aircraft, precise correlation between tunnel and flight test is not expected, however the paper delineates the major areas of confidence derived from the wind tunnel tests and shows that, for the most part, tunnel results compare favourably with flight experience. In some areas the model tests were known to be non-representative so that a degree of uncertainty remained: these areas of greater uncertainty are identified and again discussed in the light subsequent flight tests.

INTRODUCTION

Research programs relating to boundary layer control for high lift were quite common in the time period 1955 - 1965. NASA was particularly interested in the concept as applied to a possible STOL transport and modified two aircraft for research: the "Lockheed BLC Hercules" and the "Boeing 707-80". Generally speaking, it was found that the maximum lift which could be achieved by flap blowing (with just sufficient thrust to maintain attached flow) was only slightly higher than that for a good double slotted mechanical flap. Also, engine thrust loss due to compressor bleed and to the ducting, degraded takeoff performance of the projected "STOL airplane". In the light of this experience, interest was revived in jet-flap type of blowing concepts which utilize a significant proportion of total thrust in the flap and operate in the regime of supercirculation to yield much higher values of lift coefficient. It was in this context that a mutual interest was established between scientists in Canada and the U.S.A. in the augmentor flap (fig. 1) in

1963/64. It was foreseen that the penalty of duct loss could be off-set by a thrust increase generated by the augmentor flap while, at the same time, engine thrust loss could be avoided by using bypass or fan air to blow the flap in the place of compressor bleed air. In addition, the two element flap which completely shrouded the jet would ensure a very positive and substantial degree of thrust vectoring which is so essential for a steep gradient approach with landing flap setting.

These were the broad motivations but it was necessary to demonstrate many aspects of aerodynamic performance and stability before feasibility of the concept for a flight test aircraft could be established. In both countries, it was concluded that tests at large scale were essential because ejector systems were known to be sensitive to small changes in geometry and surface irregularities. Thus, in 1964, agreement was reached between NASA, Ames Research Center, the Canadian Defence Research Board and de Havilland to design and build a large scale model based on the Augmentor-Wing concept for test in the Ames 40- by 80-Foot Wind Tunnel (fig. 2). The successful outcome of these tests led to consideration of a research aircraft based on the de Havilland Buffalo airframe and using the Rolls-Royce Spey turbo-fan engine. Accordingly, in 1968, the existing large scale model was fitted with nacelles and pylons each containing a General Electric J-85 engine with vectored thrust while the tailplane height and size were adjusted to be more representative of the Buffalo aircraft. Following these modifications the model underwent a series of intensive tests in the Ames 40- by 80-Foot Wind Tunnel, with the model mounted both at the center of the tunnel and in close proximity to the tunnel floor to simulate ground reported in reference 1. Even though the layout of the research aircraft (fig. 3) was not established in detail until mid-1970, it was these model tests which formed the main source of design data.

Although many differences exist between the model and the airplane, generally it was agreed that the two were similar in all major respects so that cost of additional wind tunnel tests could be avoided. It is the purpose of this paper to show that reasonably good correlation has been found between wind tunnel, simulator and flight tests in most respects and to discuss certain areas where some real doubt existed about the predicted flight characteristics because of gaps in the design data base.

#### GEOMETRY AND CONFIGURATION COMPARISONS

General arrangement drawings of the model and the research aircraft are shown in figures 4 and 5 respectively. Some pertinent geometric data is shown in the table 1. The model is approximately a 0.55 scale of the aircraft.

The model had a wing area of 21.4 meters squared whereas the research aircraft has a wing area of 80.4 meters squared. The major differences between the model and the aircraft that would have an effect on the aerodynamics are the wing aspect ratio, 8.45 (model) compared to 7.2 (aircraft), the augmentor flap to wing chord ratio, 0.33 (model) compared to 0.24 (aircraft), the wing

dihedral, 0-degrees (model) compared to 5-degrees (aircraft), and the model ailerons were tapered whereas the aircraft ailerons were constant chord length.

The research model is powered by a turbo-compressor unit consisting of one General Electric J-85 engine, used as a gas generator to drive two modified Rolls-Royce Viper compressors. In addition, each nacelle contains one General Electric J-85 turbo-jet with diverter valve for thrust vectoring. Thus blowing thrust and nacelle thrust could be varied independently in the wind tunnel.

The research aircraft is powered by two Rolls-Royce Spey turbo-fan engines modified to collect the fan air for wing blowing and fitted with Pegasus type nozzles to vector the hot thrust. The correspondence of the "cold" blowing thrust to the "hot" vectored thrust for the modified Spey engine is shown in figure 6.

#### BASIC CORRELATION

As detailed in the previous section and table 1, some differences exist in geometry and configuration between the wind tunnel model (fig. 4) and the research aircraft (fig. 5). The performance and stability of the research aircraft were estimated prior to first flight using results from the wind tunnel as the primary source of design data with due allowance being made for these differences. Correlation is based on a comparison of the flight data with these prior estimates but, wherever possible, reference is made directly to the tunnel test results to illustrate the predicted trends and assess the degree of correlation.

The landing configuration is the more critical one from an aerodynamic point of view in nearly every respect: likewise, it is more demanding from an operational point of view. Therefore, in the present paper, consideration has been given primarily to configurations with flap angles in the range  $\delta_F = 65^\circ/75^\circ$ .

#### COMPARISONS OF MODEL AND FLIGHT DATA

Eight aspects of aerodynamics and design have been selected for discussion as follows:

- Duct loss and thrust augmentation
- Performance
- Stalling characteristics
- Ground effect
- Longitudinal stability
- Lateral stability
- Roll control power
- Flight simulation

## Duct Loss and Thrust Augmentation

The pressure loss associated with the ducting of an internally blown flap presents a source of inefficiency in this class of powered lift concept. However, one objective of the DHC/NASA program was to demonstrate that a significant quantity of air flow could be ducted to the flap without undue loss and that, in any event, an increase in thrust could be achieved in the augmentor flap which would more than off-set any thrust degradation on this account. A further objective was to demonstrate that the air-flow could be accommodated in the wing using a relatively simple ducting/nozzle combination located behind the wing spar thus leaving the main wing box essentially unaffected. This implied that the wing nozzles would be "end fed" from spanwise circular ducts rather than by fish-tail type ducting as in the case of the British jet-flap research aircraft. In general, it has been our aim to maintain the duct Mach number at less than 0.30 for choked conditions at the nozzle and then it becomes possible to maintain a fairly constant pressure along the duct (and at the nozzle) for all higher or lower values of pressure ratio.

*Duct Loss.*— The duct layout in the model is different to that in the research aircraft but the general constraints and objectives are the same, namely, to deliver about 40 percent of the engine thrust to blow the wing with a minimum of loss.

Figure 7 illustrates the loss in total pressure from the final compressor stage to the ducts which contain the wing blowing slot of the large scale model. The pressure loss is in the order of 14 percent which corresponds to a thrust loss of 9 1/2 percent. An extensively modified Viper engine was used as a compressor unit which, on account of certain design compromises, led to a significant pressure loss between the final compressor stage and the compressor plenum. Therefore a more realistic appraisal of the penalty associated with ducting can be obtained on the basis of loss between the compressor plenum and the augmentor nozzle duct. On this basis, after removing 4 percent due to the collector system, the results show a thrust loss of about 5 1/2 percent with more detailed information shown in figure 7.

A schematic of the ducting in the research aircraft is given in figure 8; also shown is the total pressure and thrust loss between the engine compressor and various points in the ducting. On the average, duct loss is less than 10 percent and the corresponding thrust loss less than 5 percent - again with more detailed information being given in the figure. Thus, achievement in this regard on the research aircraft is at least equal to that on the model in spite of the additional requirement to provide a cross-ducting capability.

*Thrust Augmentation.*— It is difficult to obtain an accurate measurement of static thrust augmentation on the research aircraft largely because of the predominant primary hot thrust of the Rolls-Royce Spey engine. However, a fully representative 7/10 scale model of the ducting system and flap was tested by Boeing during the design phase. This model, with a span of 2.4 meters, incorporated the 'twin-nozzle' arrangement as shown in figure 1. Results have been compared to half scale model of 0.38 meters span tested in the de Havilland laboratory (fig. 9).

It is important to note that nozzle loss does not appear directly as part of the system performance because thrust augmentation is defined in terms of a net gain relative to the isentropic thrust supplied to the augmentor system (where isentropic thrust is based on duct supply pressure and mass flow). The net augmentation of thrust is defined as follows: Net augmentation = Gross augmentation  $\times$  Nozzle efficiency, i.e.,  $A_{net} = A_{gross} \cdot \eta_N$  where  $A_{gross} =$  Measured augmentor thrust  $\div$  Measured nozzle thrust.

After correction to a comparable value of  $L/t$  ratio (augmentor length/nozzle thickness) the de Havilland model for flap angle  $\delta_F = 50^\circ$ , gave  $A_{gross} = 1.45$  and  $A_{net} = 1.37$  (corresponding to a nozzle efficiency of 0.94). By comparison the Boeing 7/10 scale flap model of the research aircraft gave  $A_{gross} = 1.38$  and  $A_{net} = 1.27$  (corresponding to a nozzle efficiency of 0.92). Results of tests for a range of flap angle are shown in fig. 9 in which the Boeing test data are taken from reference 2.

Both models demonstrated the capability of increasing augmentation by 4 or 5 points when operating either the upper or lower nozzle singly.

The larger scale and larger span model was unable to generate a static thrust augmentation equal to the component model in the laboratory. This experience has been fairly general throughout, whenever large scale augmentor experiments have been conducted. In part, this can be attributed to interference caused by structural members located inside the augmentor passage and due to the sensitivity of a slot nozzle ejector to such disturbances.

### Performance

Correlation has been studied for two configurations: approach and landing flap, where the ability to perform a steep descent gradient is important and takeoff flap, where climb gradient is important especially in the case of engine failure.

The appropriate aerodynamic coefficients are defined as follows:

- $C_{Lnet}$  This coefficient includes the thrust of the jet flap but excludes any lift component of hot jet reaction.
- $C_{Dnet}$  This coefficient is a measure of "drag minus thrust". It includes jet flap thrust but excludes thrust component of hot jet and momentum drag of the J-85 engines.
- $C_{J_I}$  The blowing coefficient is based on the isentropic thrust available in the wing ducts and is obtained from a knowledge of duct pressure and mass flow. It includes the blc thrust associated with the fuselage and ailerons which represents about 10 percent of the total.
- $C_{L_T}$  Total lift coefficient, including lift component of hot thrust.

There are two main differences between the wind tunnel model and the aircraft which affect performance; aspect ratio 8.45/7.2 and flap-chord ratio .33/.24 (model to aircraft respectively). Data from the model tests have been corrected for these differences according to formulae given in reference 3 and

applied to a configuration which was close to trim. The magnitude of the correction is shown in figure 10 for landing flap and found to be quite significant.

Wind tunnel performance data are obtained by running polars at constant speed and power (i.e. constant blowing coefficient). In flight, as the aircraft executes a polar at constant power, the airspeed decreases as angle of attack increases and therefore it is more difficult to obtain a set of parametric flight data. An analysis method has been used whereby  $C_{L_{net}}$  and  $C_{D_{net}}$  for a given flight polar are plotted against angle of attack; values are interpolated at constant values of  $\alpha_w$  (for each polar) and then plotted against blowing coefficient,  $C_J$ . It then becomes possible to construct lift and drag polars with  $C_J$  as parameter.

*Approach and landing flap.*— The variation of  $C_{L_{net}}$  versus  $C_{J_I}$  for  $\alpha_w = 7.5^\circ$  and for  $\alpha_w = 17.5^\circ$  are shown in figure 11. It was found that lift coefficient falls below prediction for a given  $\alpha_w$  whereas the variation with blowing coefficient (at constant  $\alpha_w$ ) follows the predicted trend quite well. It is of interest to note that "single engine" points fall in line with the two-engine data.

The drag polar is of special interest because the  $C_D$  vs  $C_L$  relationship provides a measure of descent gradient capability. Flight data show good agreement with model tests at low values of  $C_J$  (see fig. 12) but exhibit very little thrust recovery as  $C_J$  increases. Thus the flight results depart more and more from the model tests as the value of  $C_J$  increases. Generally, it is thought that thrust recovery will be realized provided the jet sheet is bent backward by the free stream before it breaks up (since after break-up it can no longer sustain a pressure differential). It is suggested that the constraint of the tunnel floor may have caused the jet sheet to bend backward sooner (for these large flap angles) and thereby some thrust recovery is achieved in the tunnel whereas, in flight, the jet sheet breaks up before being deflected streamwise. In any event the trend of the flight result is favourable, in that it permits the achievement of a steeper descent gradient.

*Takeoff flap configuration.*— The variation of lift coefficient with wing blowing thrust is shown in figure 13 for takeoff flap,  $\delta_F = 30^\circ$ . The correlation is reasonably good and somewhat better than for  $\delta_F = 65^\circ$ . The corresponding drag polars in figure 14 compare well with the estimate and indicate a similar degree of thrust recovery to that found in the tunnel. Accordingly, it was found that predictions of climb performance for takeoff flap setting agreed well with flight data and, in particular, for the single engine case.

#### $C_{L_{max}}$ and Stall Characteristics

Correlation of the stall is presented in figure 15 in terms of both maximum lift and angle of attack at which maximum lift occurs: for both  $\delta_F = 30^\circ$  and  $65^\circ$ , the maximum values of  $C_{L_{net}}$  fall slightly below the prediction based on tunnel tests. Angle of attack for maximum lift agrees well for  $\delta_F = 30^\circ$  but follows a different trend for  $\delta_F = 65^\circ$ : there is now a distinct variation

with blowing coefficient - values of  $\alpha_w$  for maximum lift are lower than predicted at low  $C_j$  and higher at high  $C_j$ . Evidently, for  $\delta F = 65^\circ$ , an increase in the blowing strength permits the wing to probe deeper into the stalled region while not generating a corresponding increase in lift.

The predicted nature of the stall has been considered in some detail in reference 4. In summary, the tunnel tests suggested that there were three predominant factors; first, the entrainment of the secondary flow into the augmentor flap provides a powerful means of boundary layer control at the mid-chord station of the wing; second, that the onset of stall occurs (quite predictably) at the wing/fuselage junction but that the disturbance is confined to the wing root because of jet entrainment; and third, that the presence and growth of this wing root disturbance causes changes in downwash at the tail to generate a post-stall pitching moment in the nose-down sense.

Lift and pitching moment characteristics for the landing configuration are given in figure 16 for the large model fitted with pylon mounted nacelles. Test results are shown at a wing blowing coefficient,  $C_j = 0.85$ , and with nacelle thrust vectored at  $90^\circ$  for three levels of thrust coefficient,  $C_T$ : 0, 0.33 and 0.82 (based on thrust from both engines). The very gentle nature of the stall is quite evident and so also is the nose-down moment which increases as the model is driven further into the post-stall region.

This behaviour may be compared with some specific flight experiments (ref. 5) with landing flap as shown in figure 17, where points in the post-stall region represent a quasi-steady state (that is to say, the pilot was able to fly the aircraft well into the post-stall region in a progressive manner). The time history shown represents a typical stall for landing flap ( $\delta F = 65^\circ$ ) with the hot jet nozzle vectored at  $67^\circ$ . In this case, the post-stall region was maintained for 6 seconds whereas, in one similar case, it was held for 16 seconds indicating a relatively docile stall as predicted. Corresponding measurements of elevator angle to trim show that up-elevator is required to hold the aircraft in the post-stall region once again following the trend established in the wind tunnel.

The same stall is shown in terms of speed variation on the right of figure 17 where the large speed margin (about 8 meters per second) and large "alpha margin" between approach and the stall (about 20 degrees) is now evident as discussed in reference 6.

The following comments made by one of the project pilots confirm these impressions and serve to illustrate some other aspects of the stall.

Flaps  $65^\circ$ , vectoring nozzles  $60^\circ$ , engine speed 95 percent maximum.

"The initial buffet was accompanied by a relatively mild roll acceleration to the left and an almost immediate shallow nose down pitch of not more than a few degrees. At pitch down, the indicated airspeed increases 6 to 8 knots very promptly, which made it difficult to continue further aft movements of the column, since  $C_{L_{max}}$  appeared to have been reached and the speed/elevator relationship was essentially post-stall. The initial left wing drop was easily limited to a bank angle of less than  $10^\circ$  by coordinated use of right

roll control and rudder and a slight forward movement of the column effected a prompt negative pitching response for recovery. When applying roll control to counter the post-buffet roll perturbation the roll control system rate limit was encountered which made it difficult for the pilot to stay in phase with the post buffet rolling motion."

Flaps 30°, vectoring nozzles 6°, engine speed 91 percent maximum.

"The predominant aspect of this stall was the fairly extreme nose high attitude reached prior to the onset of buffet. Longitudinal stability stick-fixed was more positive and a pull force was noted throughout. The maximum indicated pitch attitude reached was something in excess of 32°, and following the onset of buffet the elevator could be further applied to the aft stop, following which the aircraft demonstrated a shallow nose down pitch. No reversed response to pitch command was noted."

#### Ground Effect

Tests were conducted on the large scale model in ground effect at two heights,  $h/c = 1.3$  and  $h/c = 2.1$  for takeoff flap (50°) and landing flap (75°). For takeoff, thrust of the pod engines was directed backward in the conventional manner, whereas for the landing configuration the pod thrust was deflected downward through 85°. Data from these tests could be compared directly with corresponding data for the model mounted at the centre of the tunnel ( $h/c = 3.5$ ) where the model is essentially free of the ground plane. At a ground height of  $h/c = 1.3$  the wheels of the research aircraft would be just touching the ground with oleos extended (fig. 18).

For takeoff flap, ground effect on lift at  $h/c = 1.3$  was negligible; drag was reduced slightly and some nose down trim change was evident. Once again, it is the landing flap configuration which is critical and deserves more attention.

Even the landing flap configuration showed little ground effect on lift and drag with zero pod thrust at the highest value of  $C_J$  tested ( $h/c = 1.3$ ,  $\delta_F = 75^\circ$ ,  $C_{J_I} = 0.85$ ). It was the configuration with vectored pod thrust which introduced significant ground effect but even then, for  $h/c = 2.1$ , at moderate values of  $\alpha_w$ , the model exhibited classical ground effect trends - some increase in lift, a reduction in drag (at constant  $C_L$ ) and a change in downwash at the tail. (Not illustrated.) However, at  $h/c = 1.3$  the trend was reversed with a reduction in lift and corresponding increase in drag as shown in figure 18. This result led to serious worry with respect to the flare and touchdown characteristics which were likely to be experienced on the research aircraft.

Clearly, this adverse effect was due to impingement of hot jet on the ground and the tendency for it to deflect forward and then spill over the wing. However, there was some reason to expect that the tunnel results were pessimistic, because, first of all, the jet nozzle on the model was closer to the ground than for the research aircraft, secondly, there was a single jet at

each nacelle rather than a pair of smaller jets as on the research airplane, and thirdly, the presence of a tunnel boundary layer will always aggravate the situation by making it easier for the jet to be deflected forward against the wind stream (in the absence of a moving belt to represent the ground plane).

It was on account of these doubts that, in the initial stages of the flight trails, descent gradients were kept small and the flare manoeuvre was explored with some caution. As experience was gained it became evident that large adverse ground effects were not present and that, in some cases there appeared to be a tendency for the aircraft to float. This led to a series of tests in which the aircraft approached the runway with a very shallow descent gradient and was flown in a quasi-steady state only a few feet above the runway. Results of this investigation are shown in figure 19 (taken from refs. 5 and 6) where it can be seen that lift, drag and pitching moment all follow the classical trend and that no serious adverse ground effects are present. At touchdown, the lift is about 5 percent above the free air value.

#### LONGITUDINAL STABILITY AND CONTROL

Wind tunnel data showing lift, drag and pitching moment characteristics for the landing configuration are shown in figure 20 (tail on, elevator angle zero, nacelle thrust vectored at  $85^\circ$ ).

Certain broad conclusions could be drawn by simple inspection of the results.

- that longitudinal static stability would deteriorate as power increased, but only to a moderate extent
- that changes in trim with power (at constant speed) would be relatively small
- that an increase in power would lead to a nose-up change in trim (e.g. to facilitate wave-off)
- that elevator angle to trim would be small for steep approach at low speed.

On the left of figure 21, flight results are shown to confirm the expectations outlined above for landing flap. In particular, it is of interest to note that the aircraft is in trim with  $\delta_e = +1^\circ$  during approach at 31 to 34 meters per second, which reserves the full range of up-elevator for flare and touchdown.

Location of the engine was chosen to minimize change in trim due to nozzle vectoring for the wind tunnel model and for the research aircraft. The graph on the right hand side of figure 21 indicates that, in fact, this objective was achieved in flight.

## LATERAL STABILITY

Consideration is given to static lateral stability in general and to dihedral effectiveness in particular. A typical set of lateral data from the wind tunnel is shown in figure 22 for a landing configuration. Model tests were conducted with the addition of strakes fitted to the rear underside of the fuselage to make it more representative of the Buffalo aircraft. The model exhibited a reasonably good directional stability but the dihedral effectiveness was shown to be essentially neutral.

In contrast to zero dihedral of the model, the Buffalo aircraft has 5° dihedral over the wing panels outboard of the engine nacelles, and zero degrees for the centre section. The influence of this additional element of dihedral was completely unknown, especially, in combination with large flap angles and wing blowing. For the simulation, dihedral effectiveness was varied between the wind tunnel value  $C_{l\beta} = 0$  and a theoretically derived value  $C_{l\beta} = .004/\text{degree}$  to bracket the likely handling qualities.

Some results obtained from steady sideslip manoeuvres on the research aircraft are shown in figure 23 where it can be seen that the effective dihedral corresponds to about  $C_{l\beta} = -.003/\text{degree}$  giving the more favourable characteristics anticipated for the research aircraft due to the outboard dihedral, but nevertheless, prior to flight, this aspect of stability did represent one of the major elements of uncertainty.

Making reference to the same figure it can be seen that directional stability is close to prediction and that the overall characteristic is to give approximately one degree of rudder per degree of sideslip with the condition remaining quite linear out to  $\pm 15^\circ$  of sideslip - this observation again relating to the landing configuration.

## ROLL CONTROL POWER

The approach and touchdown speed of the research aircraft is about 20 kt. below that of a standard Buffalo aircraft: nevertheless the size and control power of both the horizontal and vertical tail were considered to be adequate (the cross-ducting being a major consideration in this regard). However, it was recognized that a significant increase in roll control power would be required to give satisfactory handling qualities at low speed and, accordingly, special attention was given to this requirement during the wind tunnel test program. A roll control system was devised which consisted of three elements, a blown aileron, a spoiler located just ahead of the aileron and a small flap which reduced the exit area of the augmentor flap in a region outboard of the engine nacelle. This latter control became known as the augmentor choke.

A typical set of data taken from the wind tunnel (fig. 24) shows the characteristics and relative effectiveness of each element. Individually it

can be seen that each form of control holds effectiveness throughout the complete range of  $C_L$  and each is reasonably linear over the range of control tested. In addition, tests were carried out with the various controls in combination to assess interference effects. These rolling moment characteristics were used by Boeing in the design of a powered control system (using all three elements) to generate the set of flight data shown in figure 25, giving a high degree of sensitivity about neutral control deflection and high rates of acceleration for maximum control. Maximum control deflections chosen for the research aircraft were ailerons  $\pm 15^\circ$ , spoilers -  $50^\circ$  and chokes 55 percent.

Correlation of roll control power between tunnel and flight is illustrated in the same figure by a single point prediction based on data from reference 5 at maximum wheel angle. It is evident that the flight result came close to expectation in this respect.

Although not relating to correlation, an important design feature of the research aircraft is that blowing air is cross-fed to the wing so as to minimize moment imbalance due to vectored thrust in the event of engine failure. In the approach configuration, roll imbalance is very small so that maximum control power is available for manoeuvre and for SAS actuation. For takeoff, engine out yawing moments are compensated so as to permit takeoff on one engine from a standing start.

#### FLIGHT SIMULATION TESTS

Slight simulation was carried out during the design phase on the large six-degree of freedom moving base unit at the Ames Research Center known as the "Flight Simulator for Advanced Aircraft" (ref.7). Wind tunnel test data from the large scale model provided the main source of aerodynamic derivatives and characteristics for the simulation whereas rotary derivatives were estimated theoretically. Variations in ground effect and dihedral effectiveness were introduced to bracket the degree of uncertainty in these two parameters. The cockpit of the simulator was modified to make it closely representative of the Buffalo aircraft with regard to the instrument panel and location of controls. In particular, a nozzle control lever for thrust vectoring was located right along side of the overhead throttles of the standard Buffalo.

The handling and control of the research aircraft was examined for all operating modes such as, approach, flare and touchdown, transition and glide path intercept, single engine failure, etc., and, over a wide range of atmospheric conditions such as wind shear, cross-wind and turbulence.

In retrospect it can be said that the simulator provided a reasonably close approximation to the control and handling qualities of the research aircraft. In fact, following the initial flight, one of the first comments by T. Edmonds (Chief Boeing pilot) was to the effect that "the airplane flew well at all speeds with handling qualities similar to those experienced on the simulator". Subsequent experience has confirmed this view with the exception of the landing manoeuvre. It is well known that flare and touchdown always prove difficult to simulate for a variety of reasons; the situation was

aggravated by the adverse ground effects dictated by results of the wind tunnel tests. Even with zero ground effect set up on the simulator, flare and touchdown was not easy. As described earlier, flight experience revealed a favourable ground effect which resulted in a more accurate and gentle touchdown on the aircraft than was experienced on the simulator.

Earlier indications from analysis of flight results suggest that the estimation of rotary derivatives was reasonably good - in all probability, this contributed significantly to the success of the simulation.

### CONCLUSIONS

Data collection and analysis of wind tunnel and flight experiments are more difficult for a powered lift type of aircraft because of the introduction of blowing coefficient as an additional major parameter and because of the powerful influence of thrust vectoring on performance. Notwithstanding these difficulties, many aspects of aerodynamic performance and stability have been investigated and a reasonable level of correlation has been demonstrated between wind tunnel and flight test data.

In areas where some uncertainty did exist because of gaps in the design data base of differences in geometry, the research aircraft has come out mostly on the good side of the ledger. This must be attributed partly to good fortune.

### ACKNOWLEDGEMENTS

The authors wish to express their appreciation for assistance in analysis of flight test and wind tunnel data from H. C. Quigley of NASA, Ames Research Center and from K. A. J. Lockwood and J. E. Farbridge of de Havilland (Canada).

The wind tunnel and flight test work reported here form part of an international research program funded by the National Aeronautics and Space Administration, the Canadian Defence Research Board and the Department of Industry, Trade and Commerce of Canada (DITC).

#### REFERENCES

1. Cook, A. M.; and Aiken, T. M.: Low-Speed Aerodynamics Characteristics of a Large-Scale STOL Transport Model with Augmented Jet Flaps. NASA TM X-62,017.
2. Ashleman, R. H.; and Shavdahl, H.: The Development of an Augmentor-Wing Jet STOL Research Airplane, Volume 1 - Summary. NASA CR-114503, August 1972.
3. Williams, J.; Butler, S. F. J.; and Wood, M. N.: The Aerodynamics of Jet Flaps. Royal Aircraft Establishment, Report no. Aero 2646.
4. Whittle, D. C.: The Augmentor-Wing Research Program, Past, Present and Future, AIAA Paper #67-741.
5. Quigley, Hervey C.; and Innis, Robert C.: A Flight Investigation of the STOL Characteristics of an Augmented Jet Flap STOL Research Aircraft. NASA TM X-62-334.
6. Cook, W. L.; Hickey, D. H.; and Quigley, H. C.: Aerodynamics of Jet Flap and Rotating Cylinder Flap STOL Concepts. AGARD Fluid Dynamics Panel. Paper no. 10, June 24, 1974.
7. Quigley, H. C.; and Holzhauser, C. A.: Requirement for Simulation in V/STOL Research Aircraft Programs. AGARD Fluid Dynamics Panel. Paper no. 25, June 24, 1974.

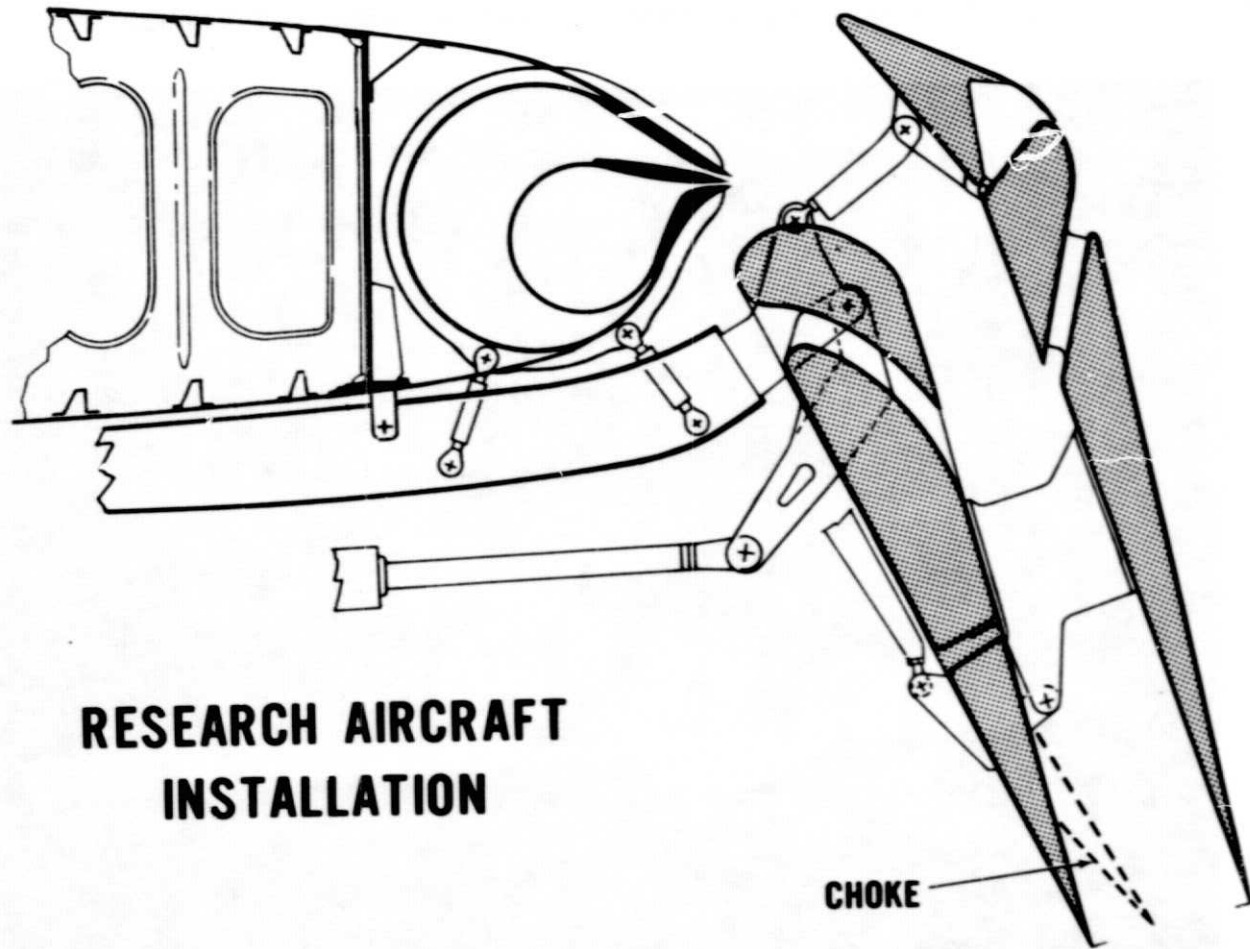
TABLE 1.- MOL AND RESEARCH AIRCRAFT GEOMETRY

	Wind Tunnel Model	Research Aircraft
Wing		
Gross area, sq. m	21.37	80.36
Span, m (B)	13.46	24.0
Aspect ratio	8.45	7.2
Root chord, m	1.73	3.77
Tip chord, m	0.81	2.36
Thickness/chord ratio	.16	.175 - .15
Dihedral angle	0	5.0
Flap		
Chord, m (aft of hinge line)	.56	.91
Chord ratio	.33	.24
Span, m	3.72	7.01
Semi-span location $k(b/2)$	.12 - .67	.12 - .72
Aileron		
Root chord, m (aft of hinge line)	.4	.61
Tip chord, m	.24	.61
Span, m	1.72	3.50
Semi-span location $k(b_2)$	.68 - 1.0	.72 - 1.0
Spoiler		
Chord, m	.17 - .10	.36
Span, m	1.52	3.44
Semi-span location $k(b/2)$	.73 - .96	.72 - .99
Horizontal Tail		
Area, sq. m	5.92	21.65
Span, m	5.27	9.75
Aspect ratio	4.68	4.4
Tail arm, m	7.25	14.11
Tail height, m (relative to wing)	2.42	5.0
Tail volume, $\bar{V}_H$	1.16	1.0
Vertical Tail		
Area, sq. m	3.9	14.1
Span, m	2.30	4.14
Aspect ratio	1.37	1.2
Tail arm, m	6.25	13.23
Tail volume, $\bar{V}_V$	.085	.097

TABLE 1.- MODEL AND RESEARCH AIRCRAFT GEOMETRY - Concluded

	Wind Tunnel Model	Research Aircraft
Angular Settings		
Wing incidence, deg (relative to fuselage)	0°	+2.5°
Wing dihedral, deg (outer panels only)	0°	+5.0°
Horizontal tail setting, deg (relative to fuselage)	-4°	+1.0°

PRECEDING PAGE BLANK NOT FILMED



## RESEARCH AIRCRAFT INSTALLATION

Figure 1.- Augmented Jet Flap

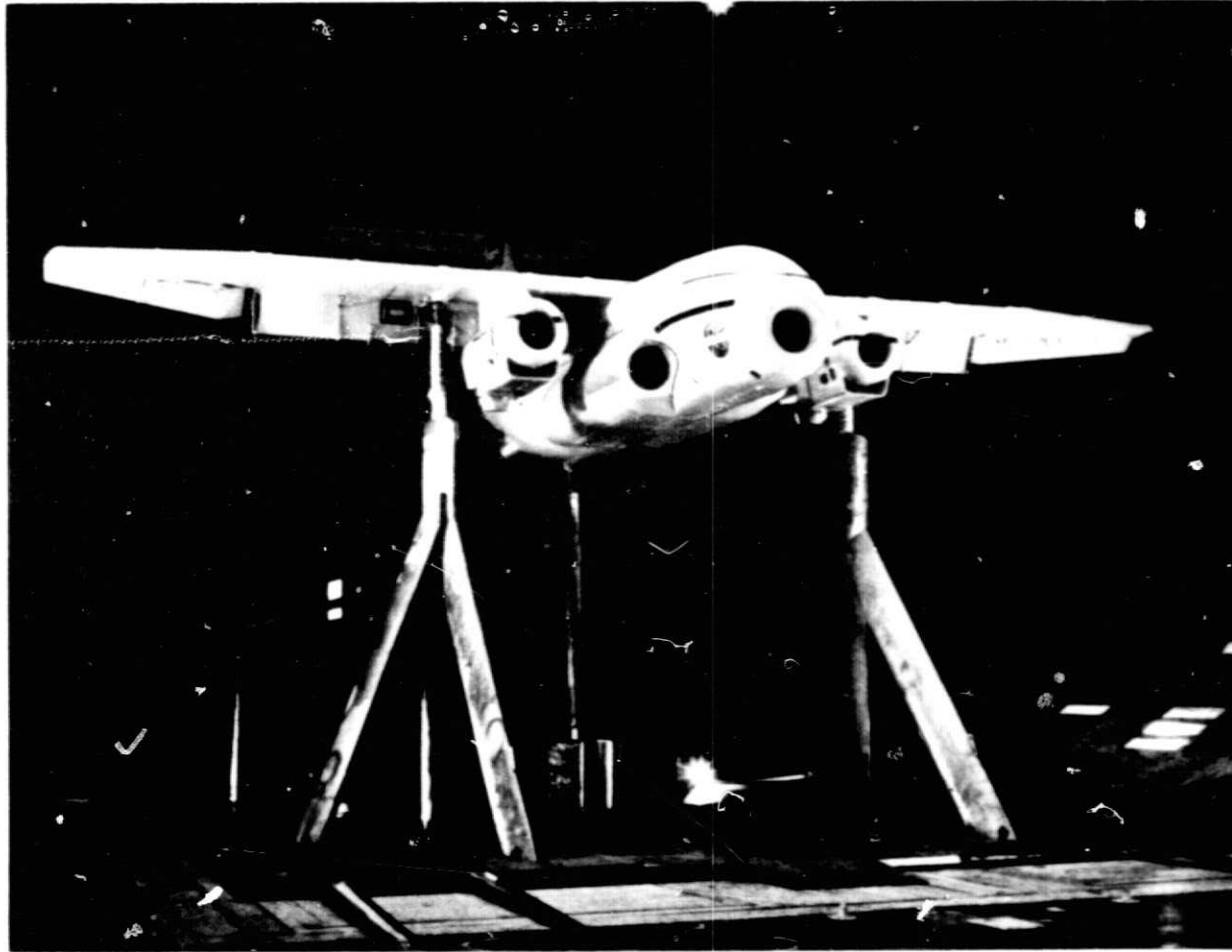


Figure 2.- Augmented Jet Flap Research Wind Tunnel Model.



Figure 3.- Augmented Jet Flap STOL Research Aircraft.

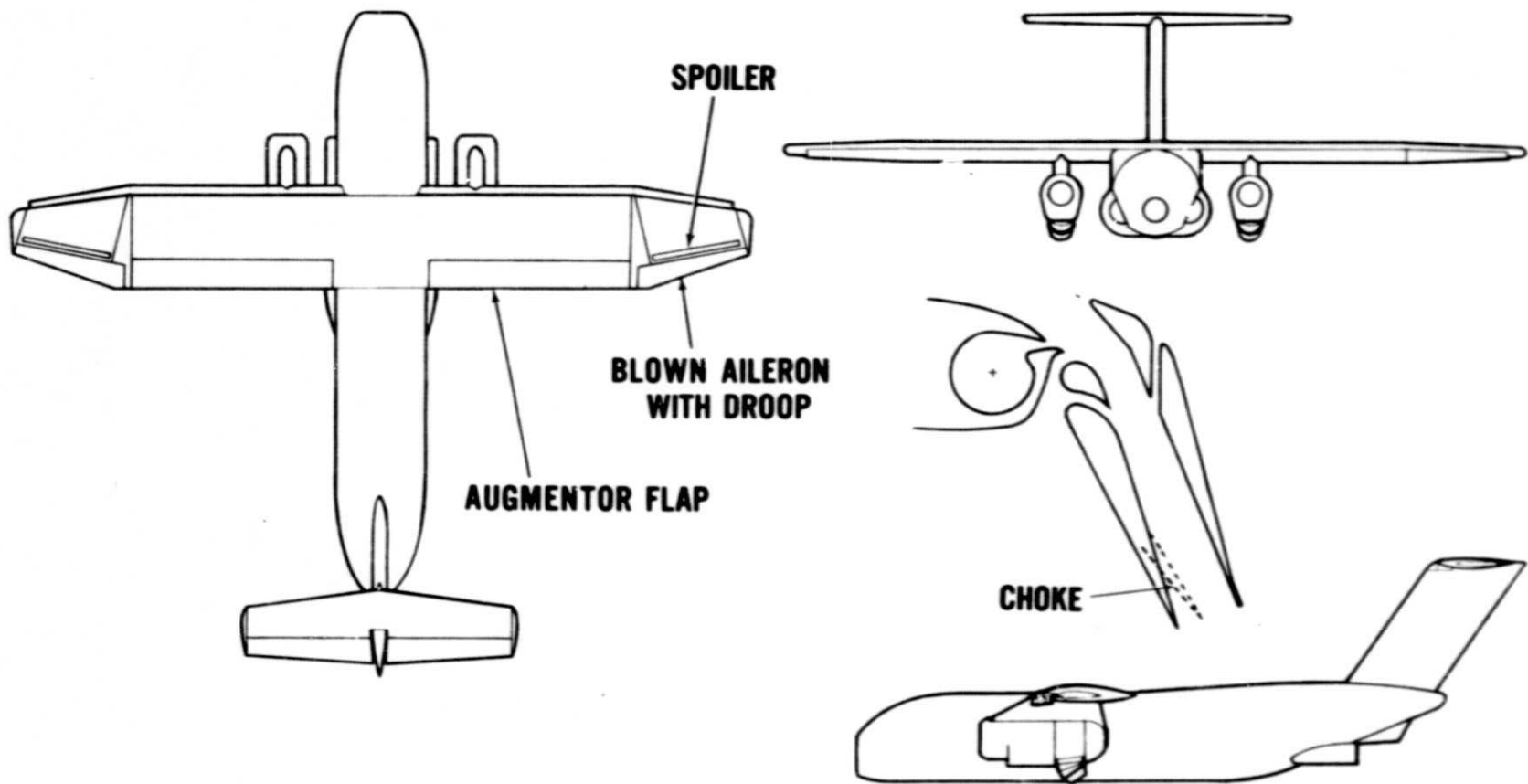


Figure 4.- Augmented Jet Flap Research Wind Tunnel Model. Three View.

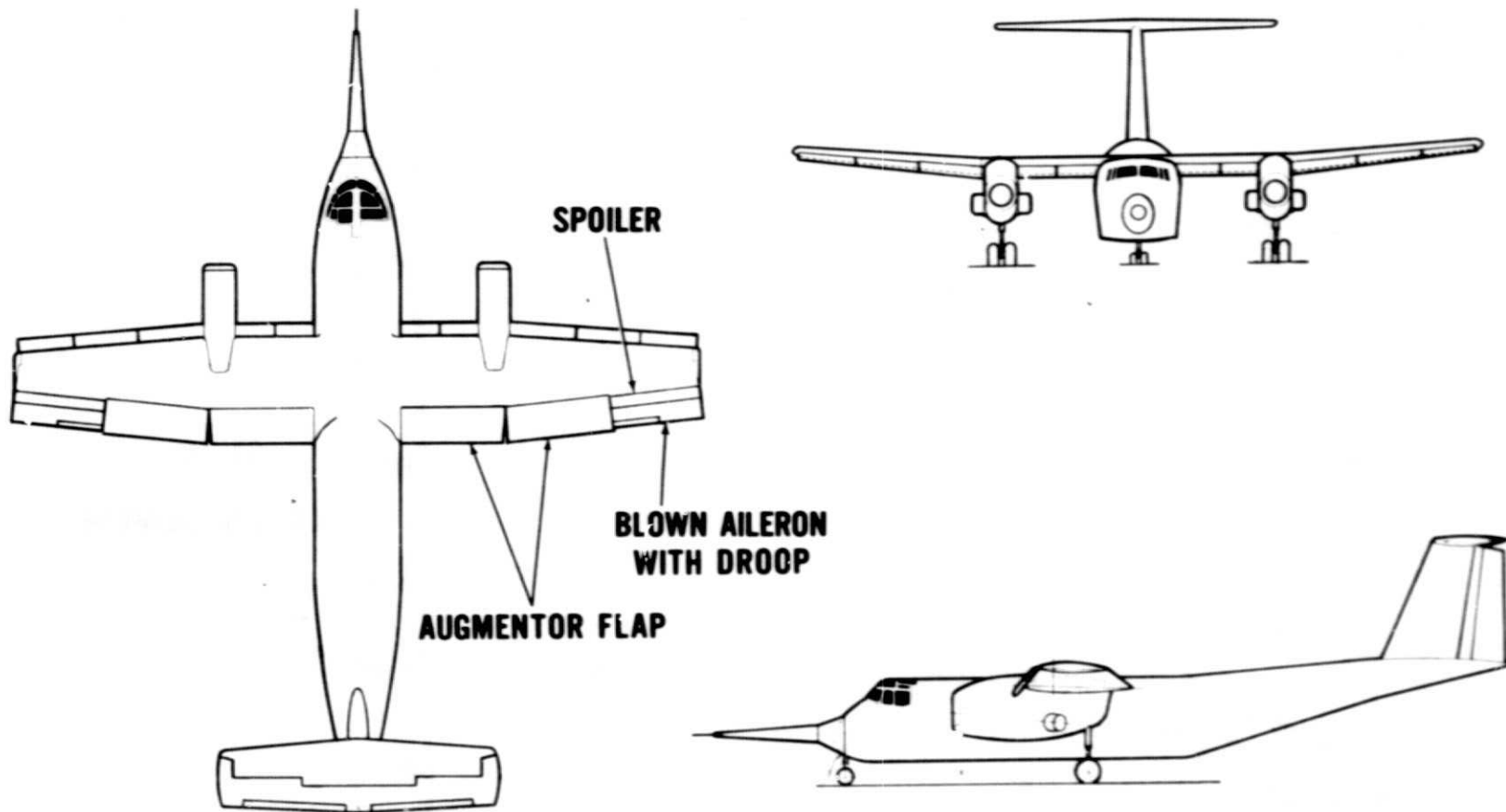
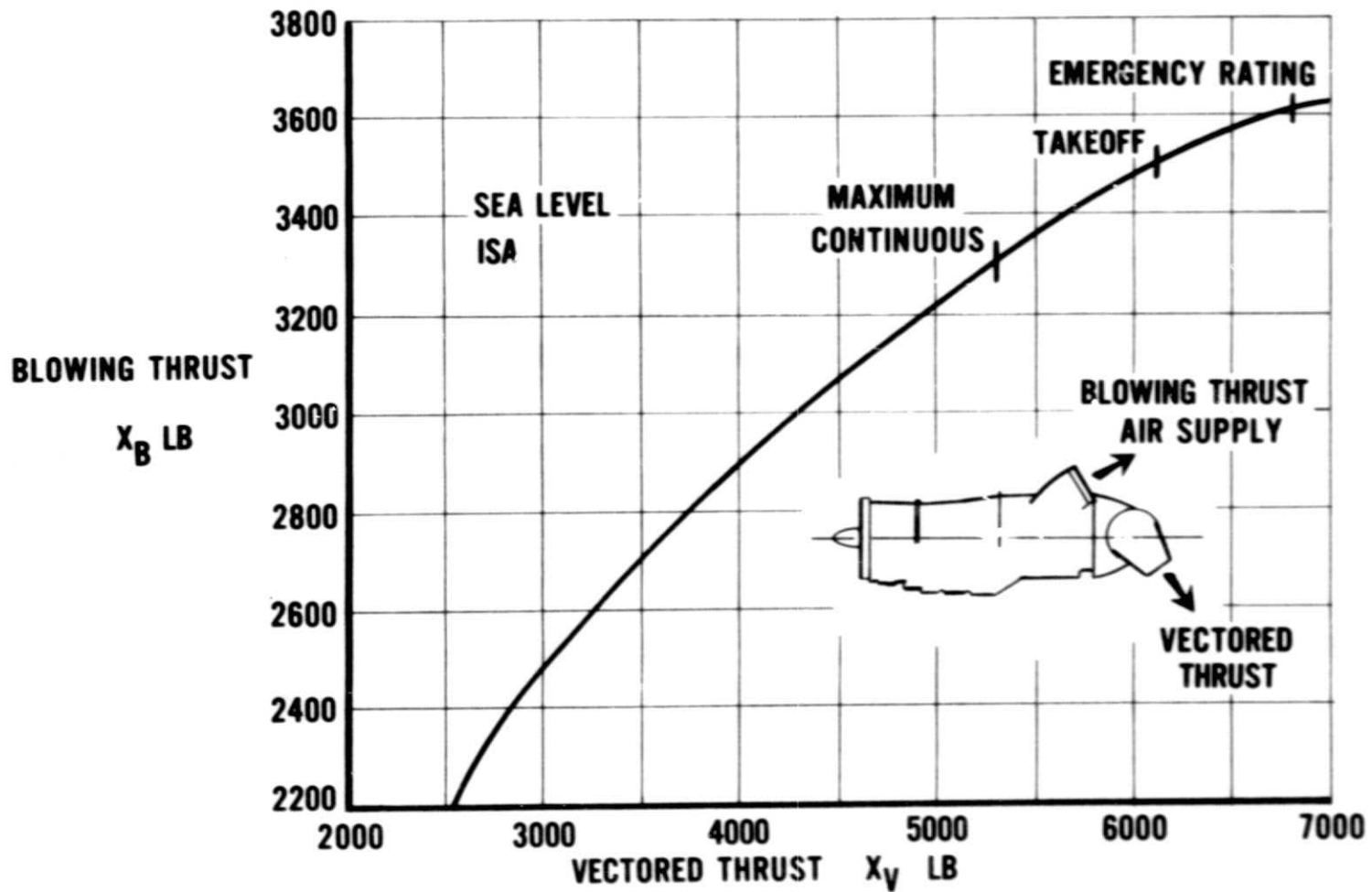


Figure 5.- Augmented Jet Flap STOL Research Aircraft. Three View.



CONVERSION: 0.454 LB = KILOGRAMS

Figure 6.- Performance of Modified Spey Turbo-Fan Engine.

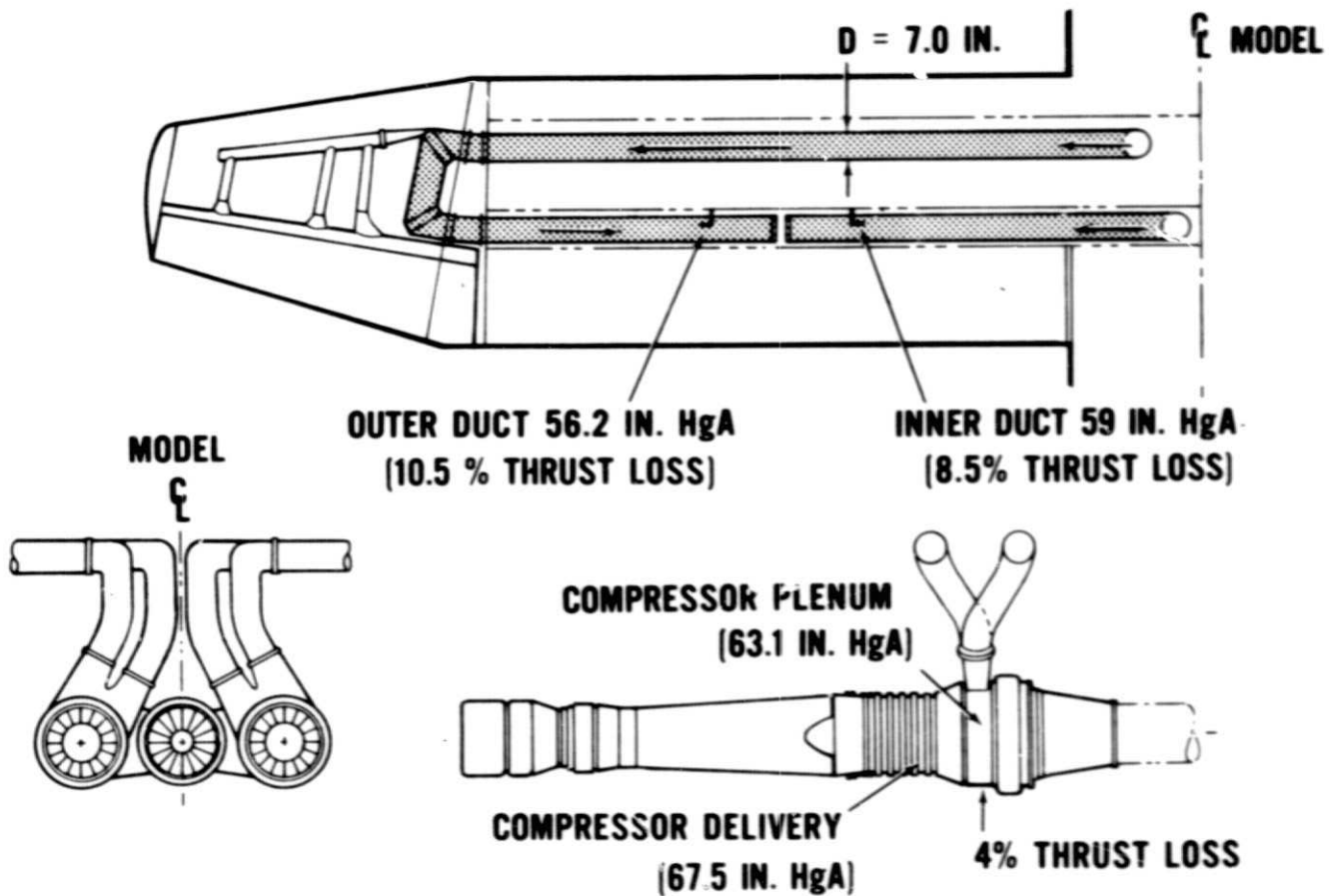


Figure 7.- Wind Tunnel Model Turbo-Compressor and Wing Ducting.

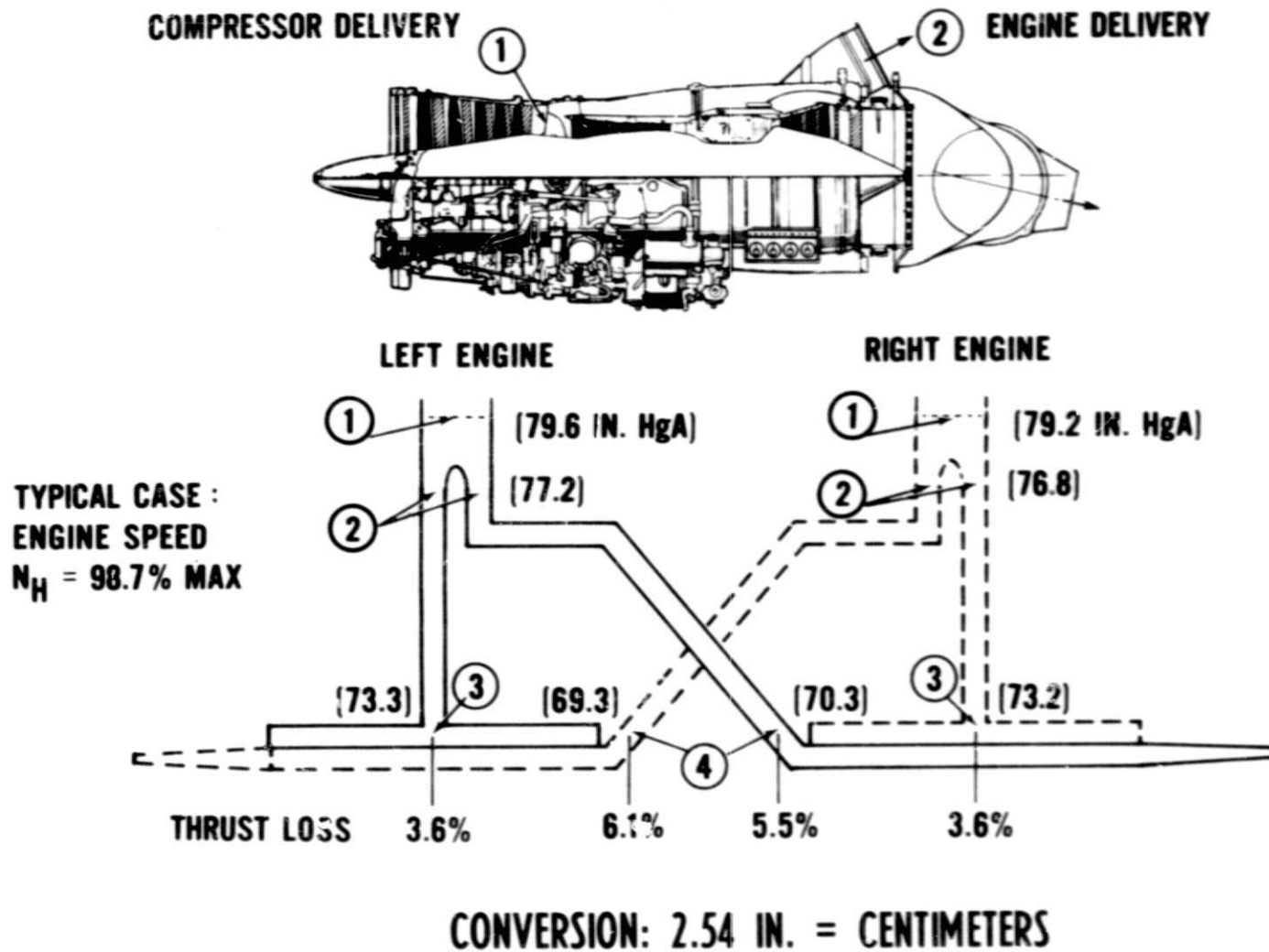


Figure 8.- Research Aircraft Spey Engine and Wing Ducting.

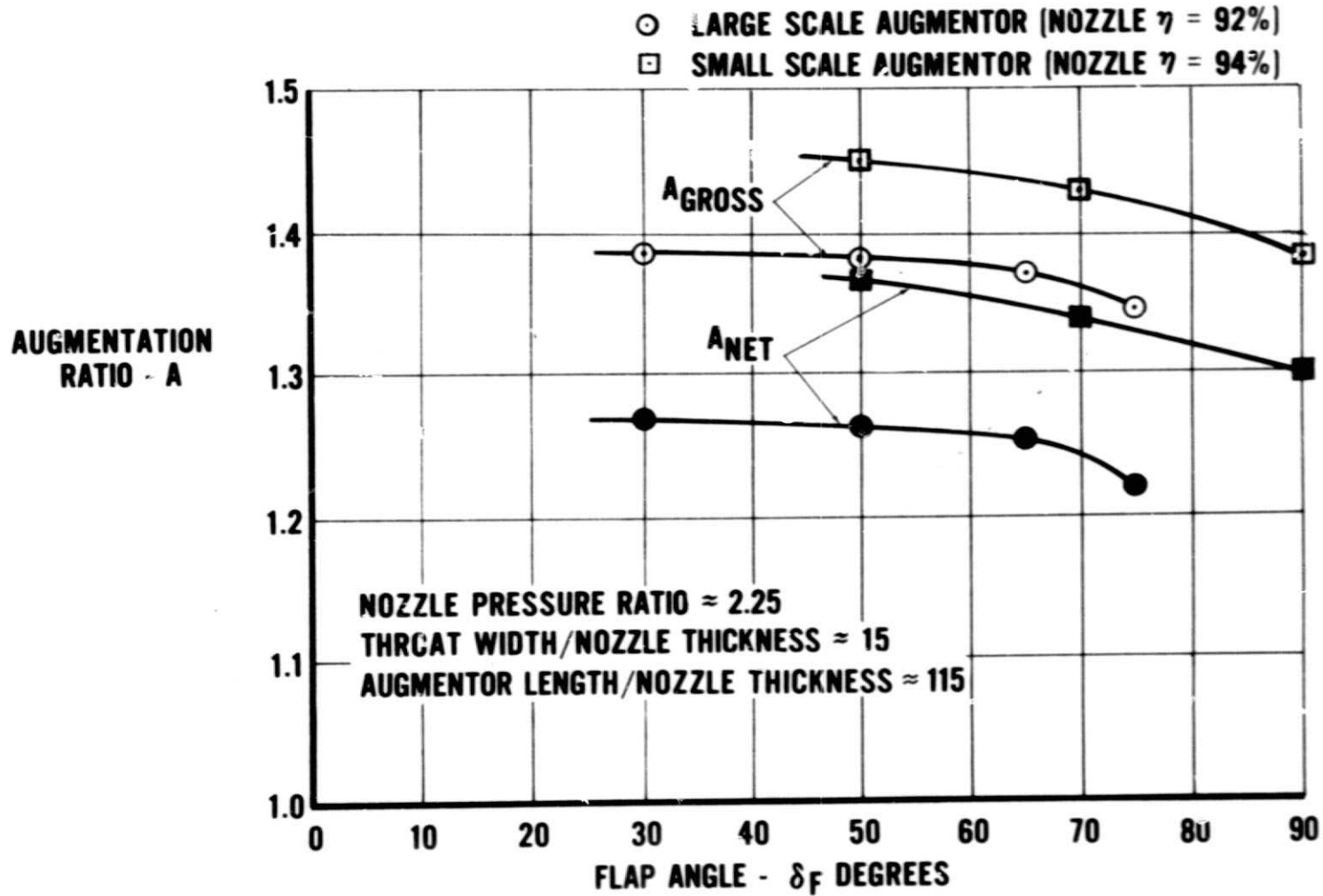


Figure 9.- Thrust Augmentation Ratio Measurements.

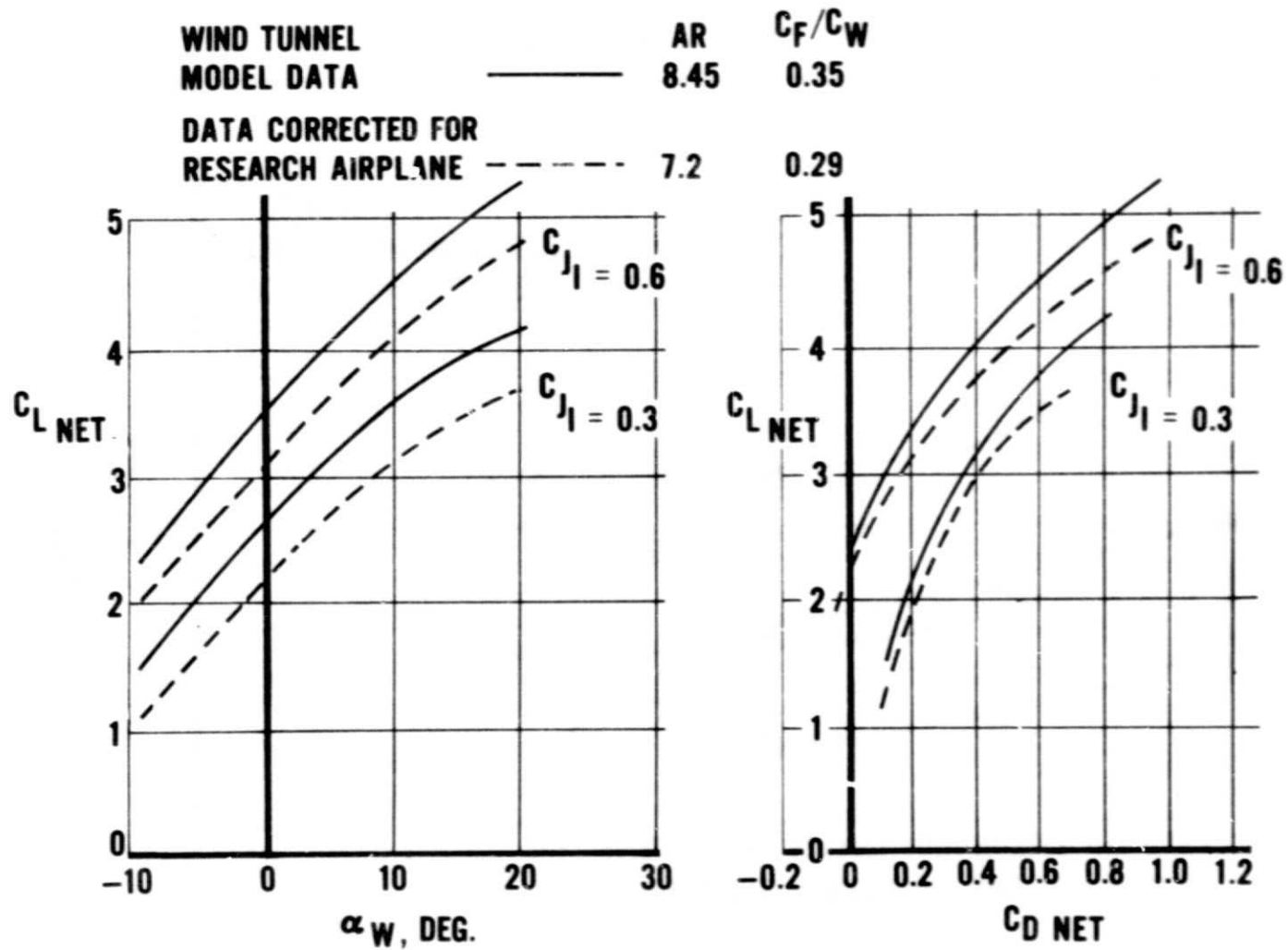


Figure 10.- Model Lift and Drag Polars.  $\delta_F = 65^\circ$ .

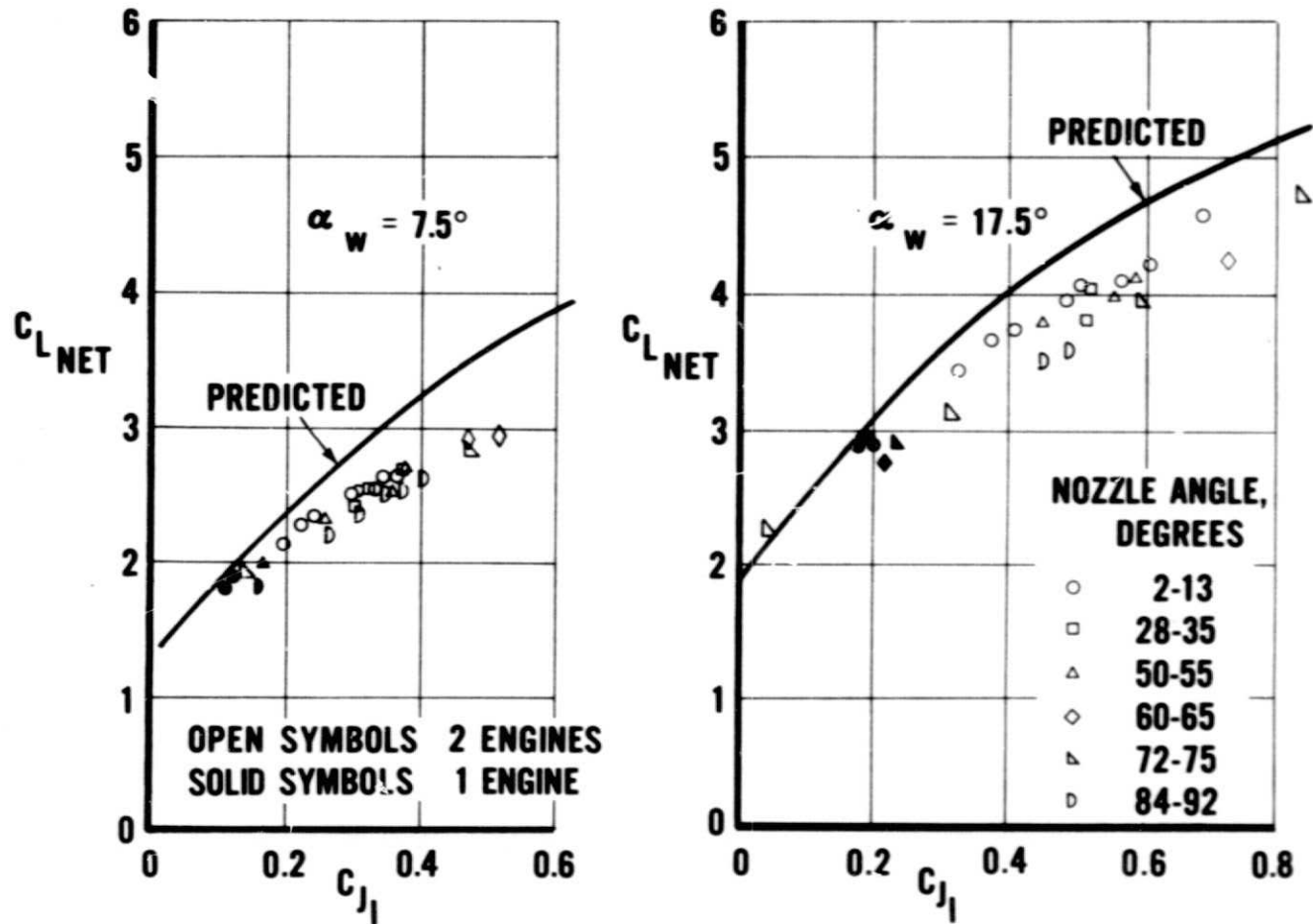


Figure 11.- Comparison of Lift Coefficient due to Blowing.  $\delta_F = 65^\circ$

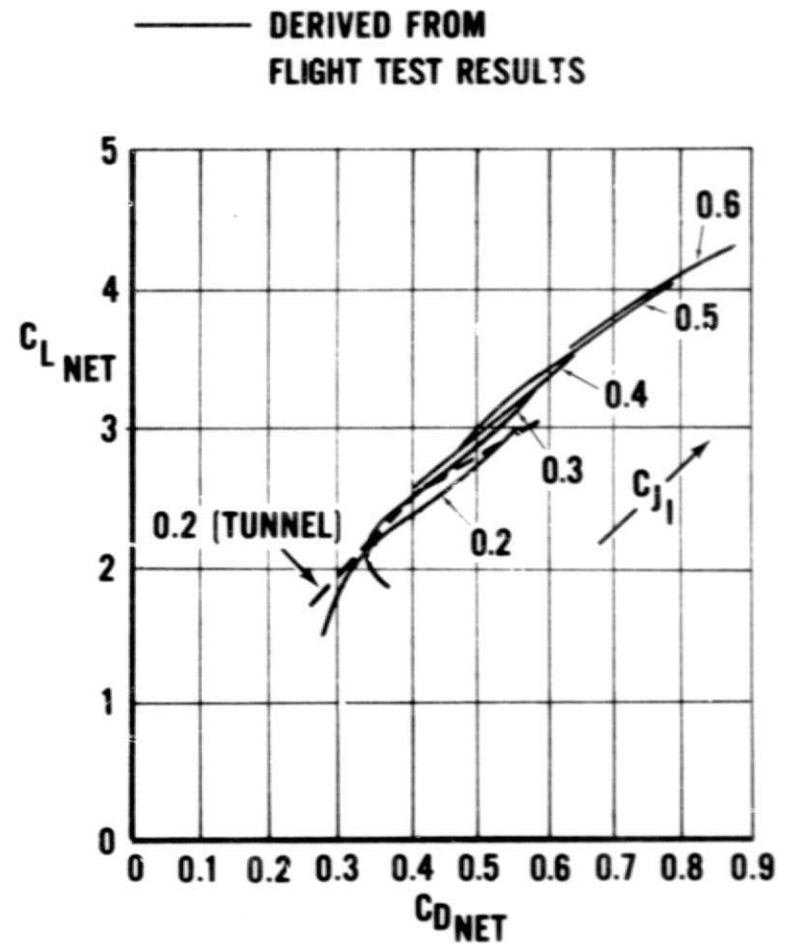
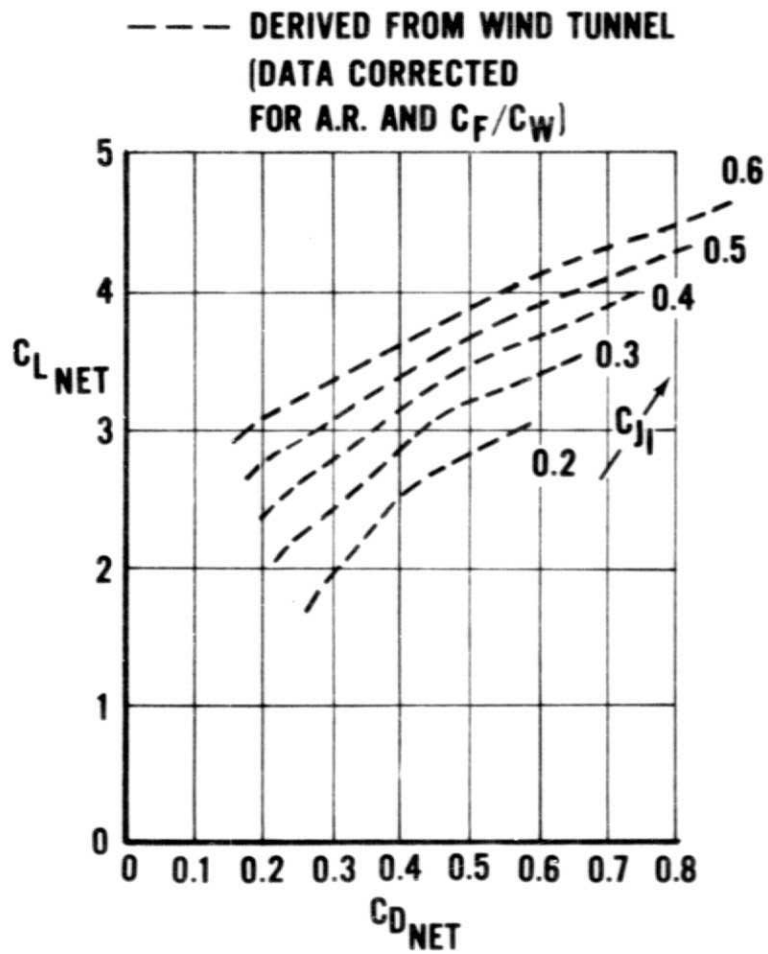


Figure 12.- Comparison of Drag Polars.  $\delta_F = 65^\circ$

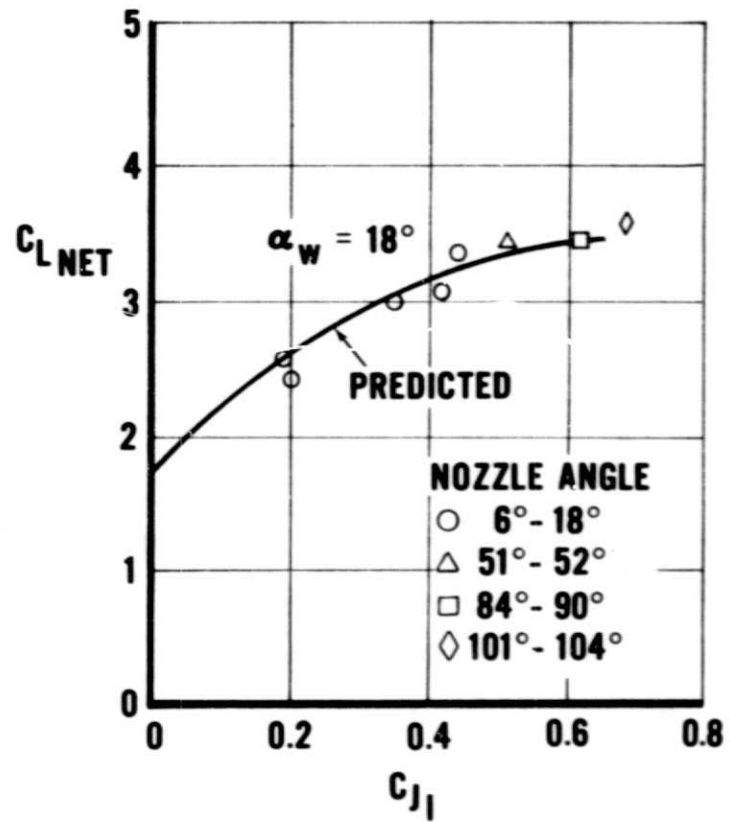
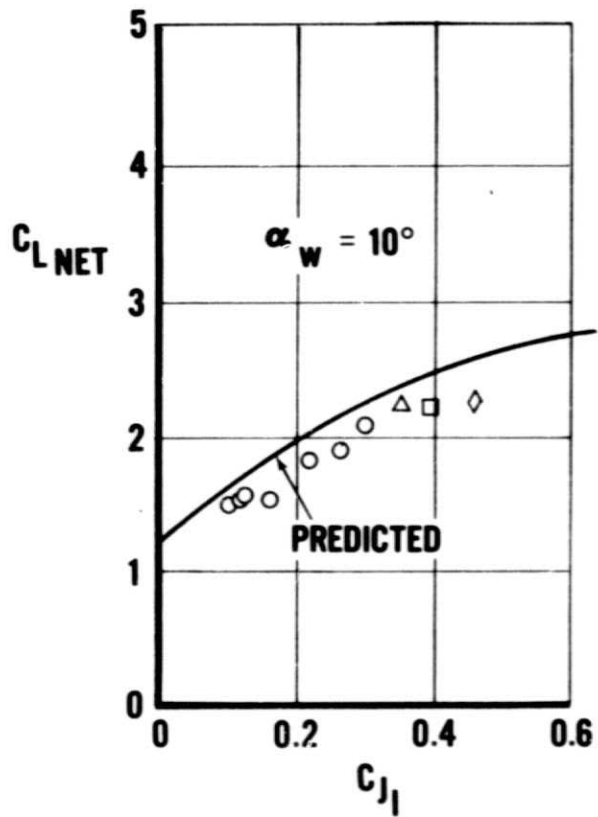


Figure 13.- Comparison of Lift Coefficient due to Blowing.  $\delta_F = 30^\circ$ .

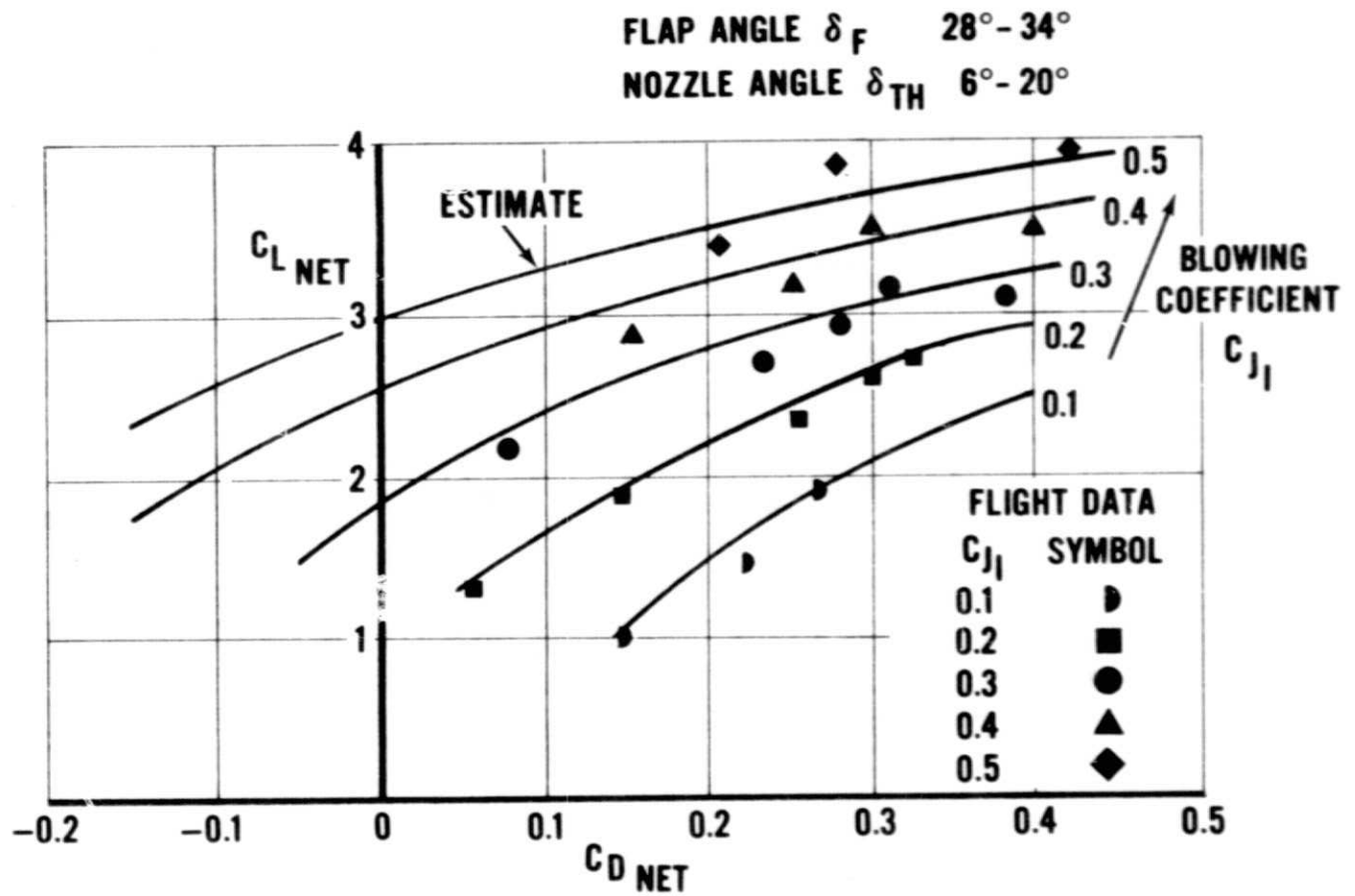


Figure 14.- Comparison of Drag Polars.  $\delta_F = 30^\circ$ .

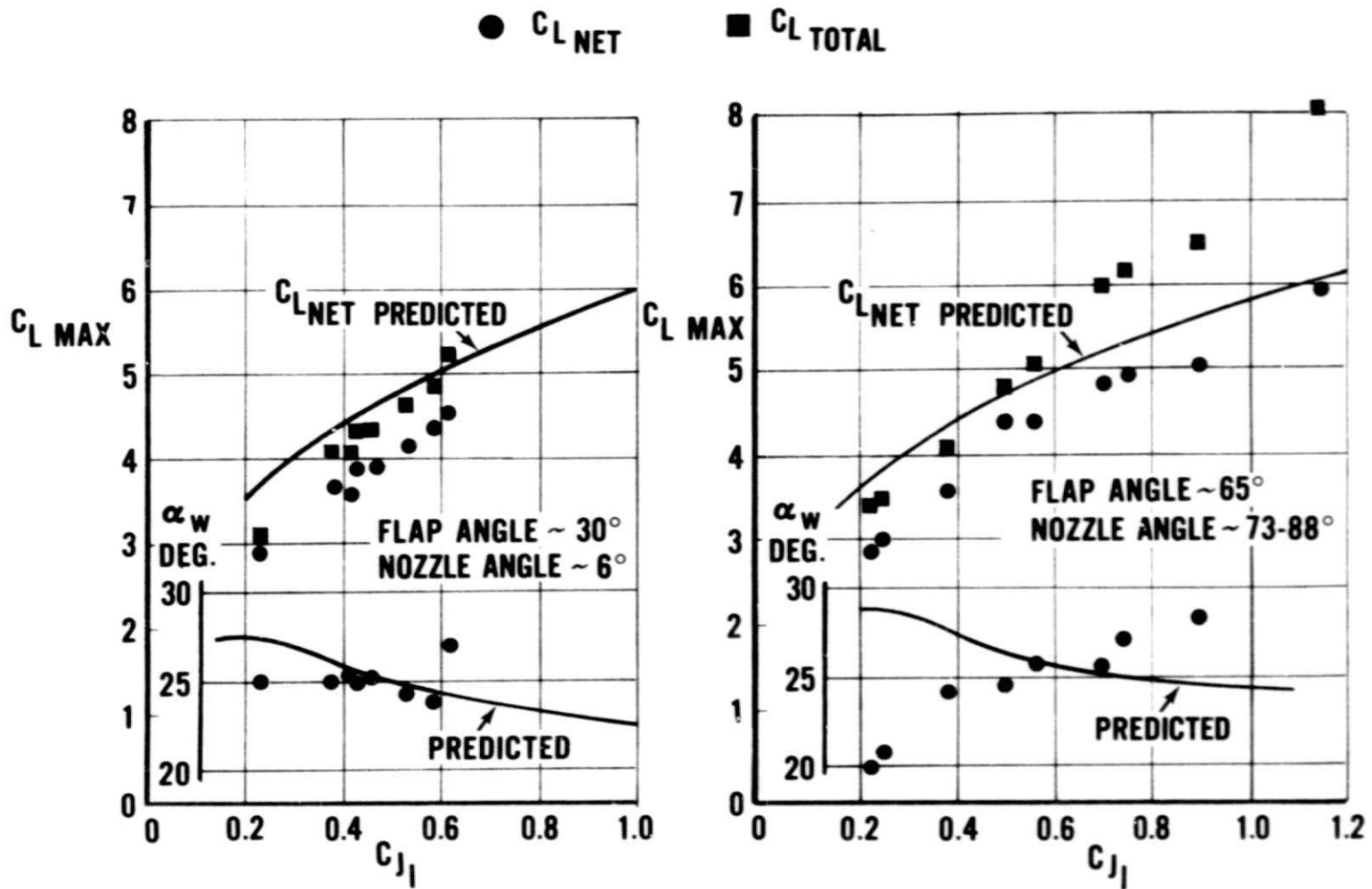
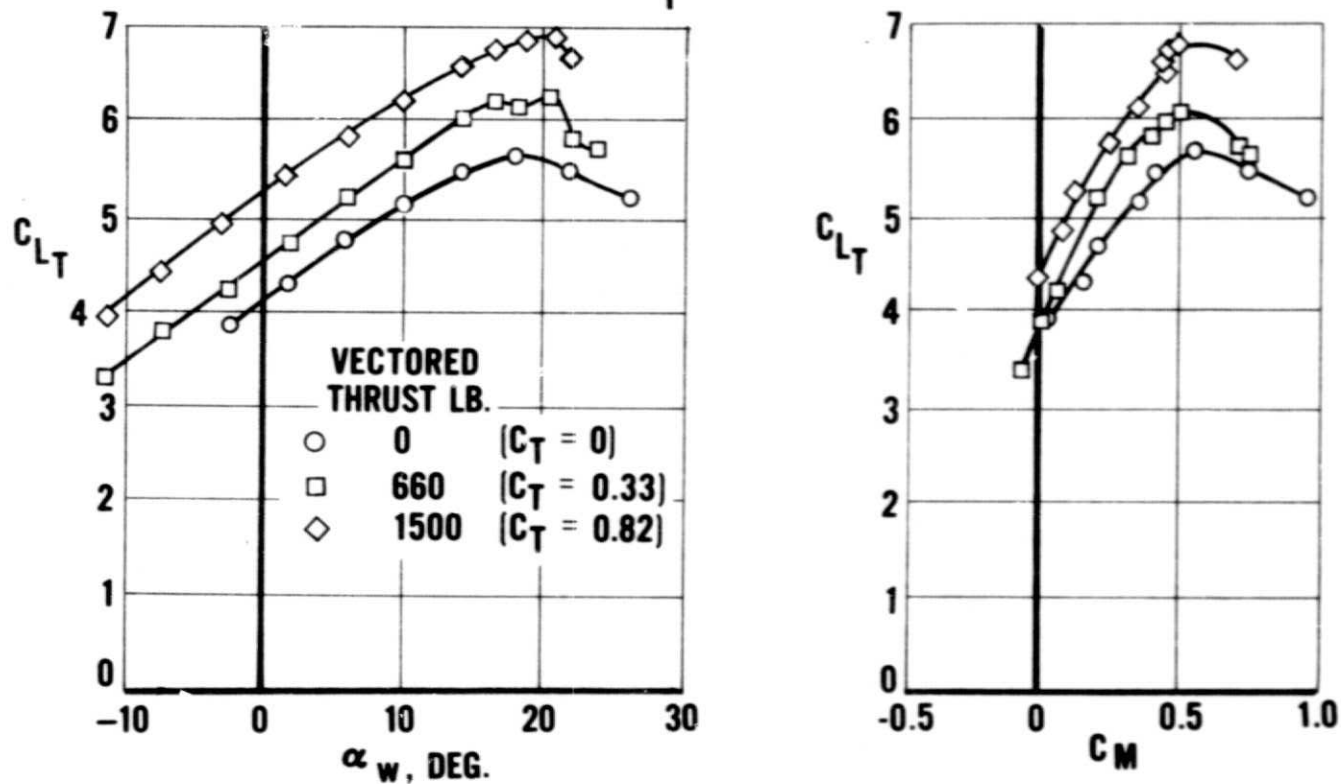


Figure 15.- Comparison of Maximum Lift Performance.

FLAP ANGLE  $75^\circ$   
 NOZZLE ANGLE  $85^\circ$   
 WING  $C_{J_1}$  0.85

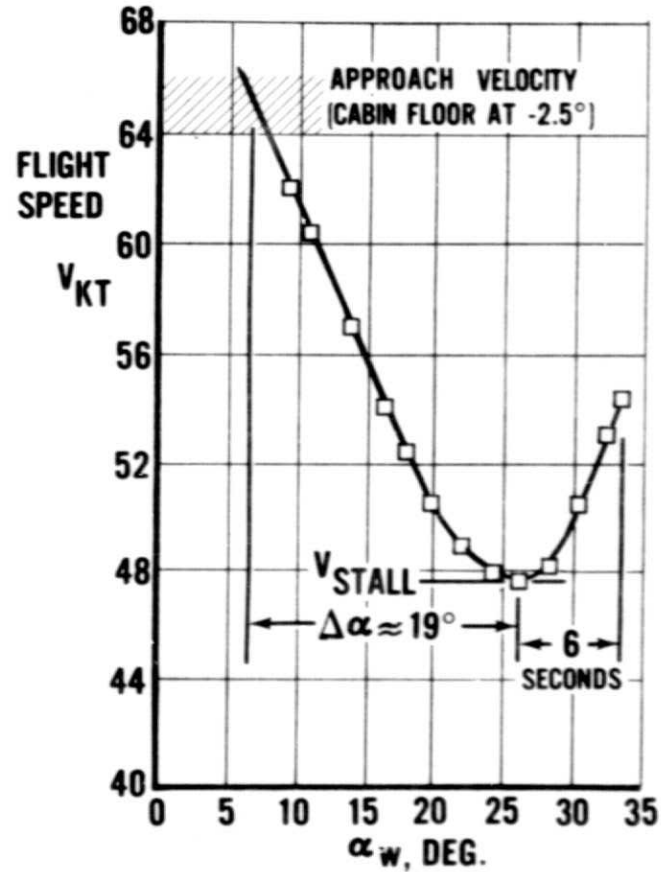
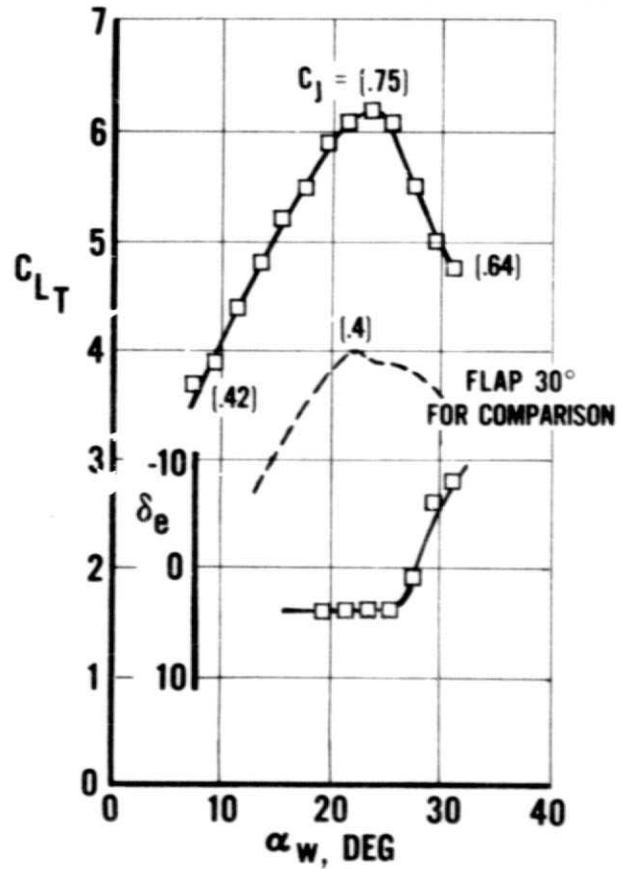


CONVERSION: 0.454 LB = KILOGRAMS

Figure 16.- Model Lift and Pitching Moment Showing Penetration of Stall.

**FLAP ANGLE 65°**  
**NOZZLE ANGLE 67°**  
**ALTITUDE ≈ 6000 FT (1830M)**

**ENGINE SPEED ( $N_H$ ) 95.9%**  
**WEIGHT 42,900 LB (19,500Kg)**



**CONVERSION: 0.454 LB = KILOGRAMS**

Figure 17.- Research Aircraft Flight Stall Behavior.



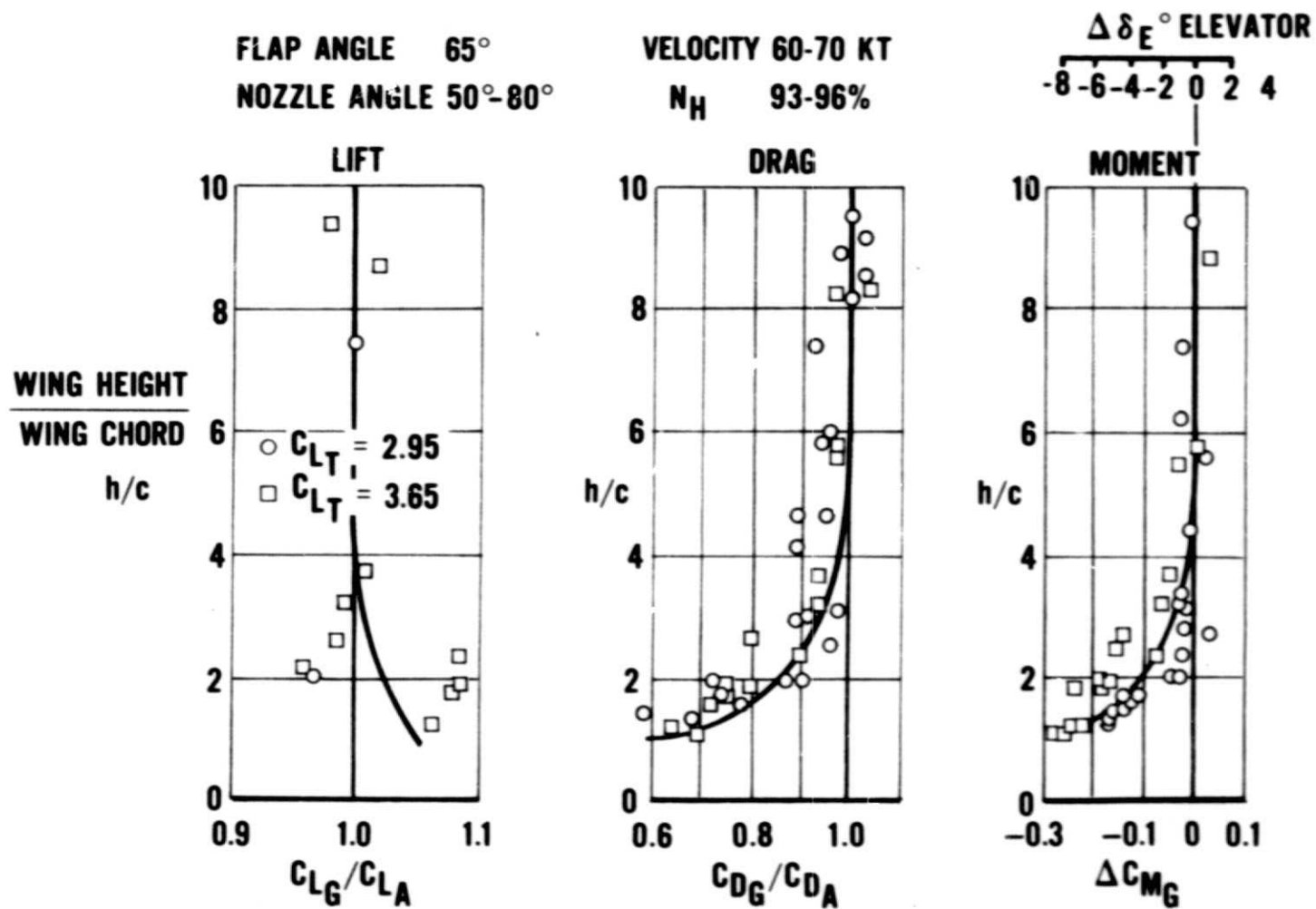


Figure 19.- Effect of Ground. Research Aircraft Flight Test.

FLAP ANGLE - 75°, NOZZLE ANGLE - 95° ( $C_T = 0.82$ ), TAIL ON

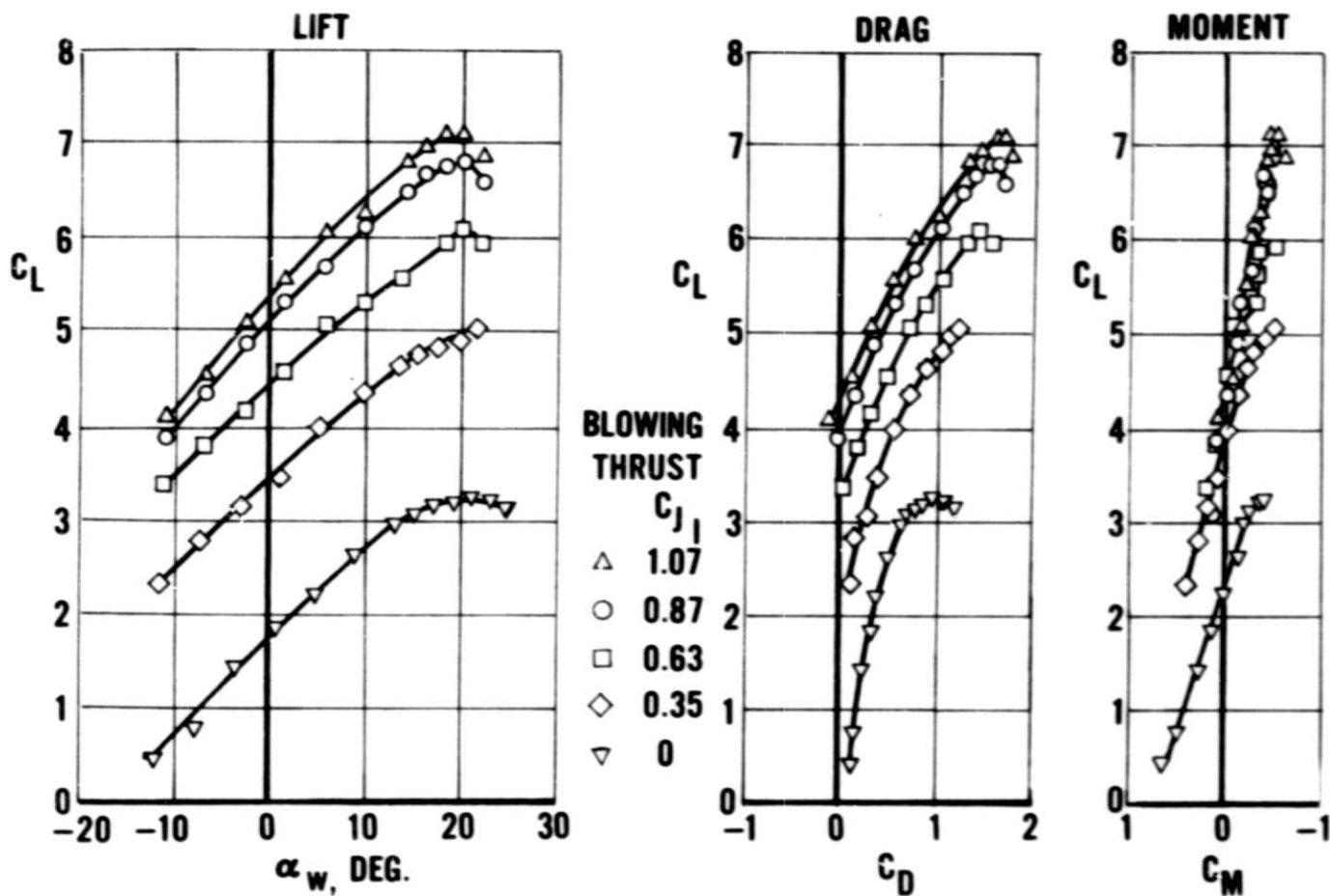
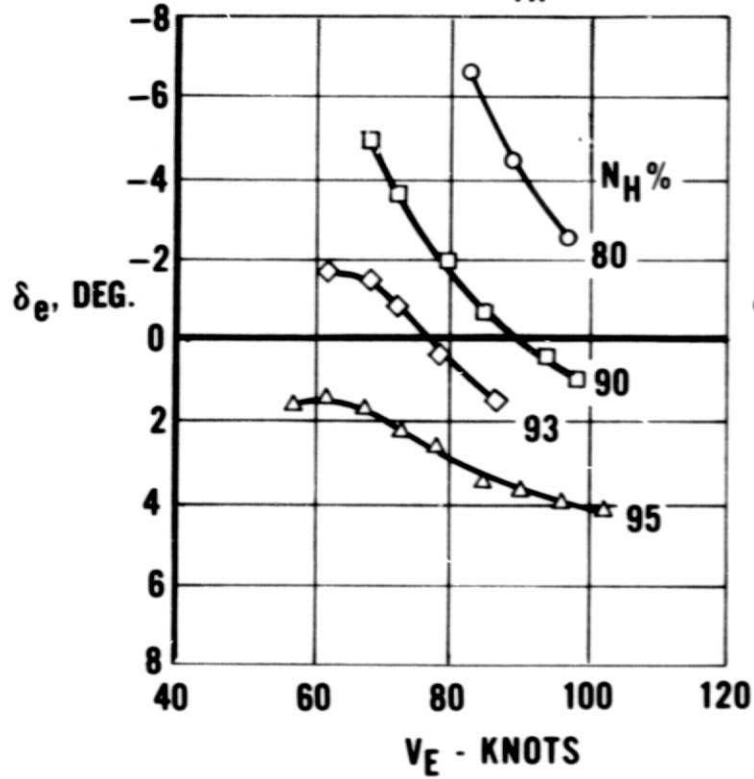


Figure 20.- Longitudinal Characteristics. Wind Tunnel Model Tests.

### ENGINE POWER

FLAP ANGLE  $\delta_F = 67^\circ$   
 NOZZLE ANGLE  $\delta_{TH} = 10^\circ$



### NOZZLE ANGLE

FLAP ANGLE  $\delta_F = 67^\circ$   
 ENGINE SPEED  $N_H = 95\%$

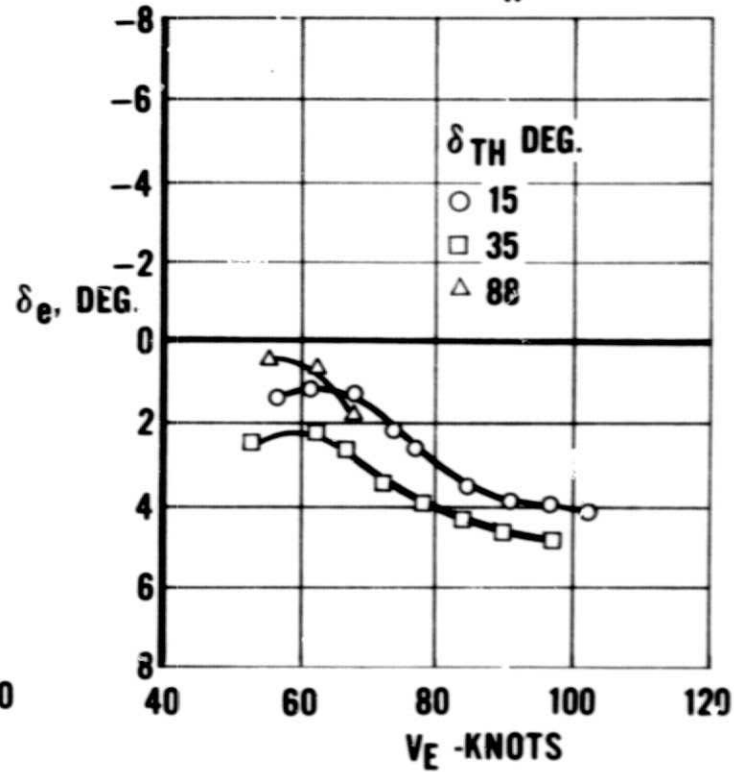
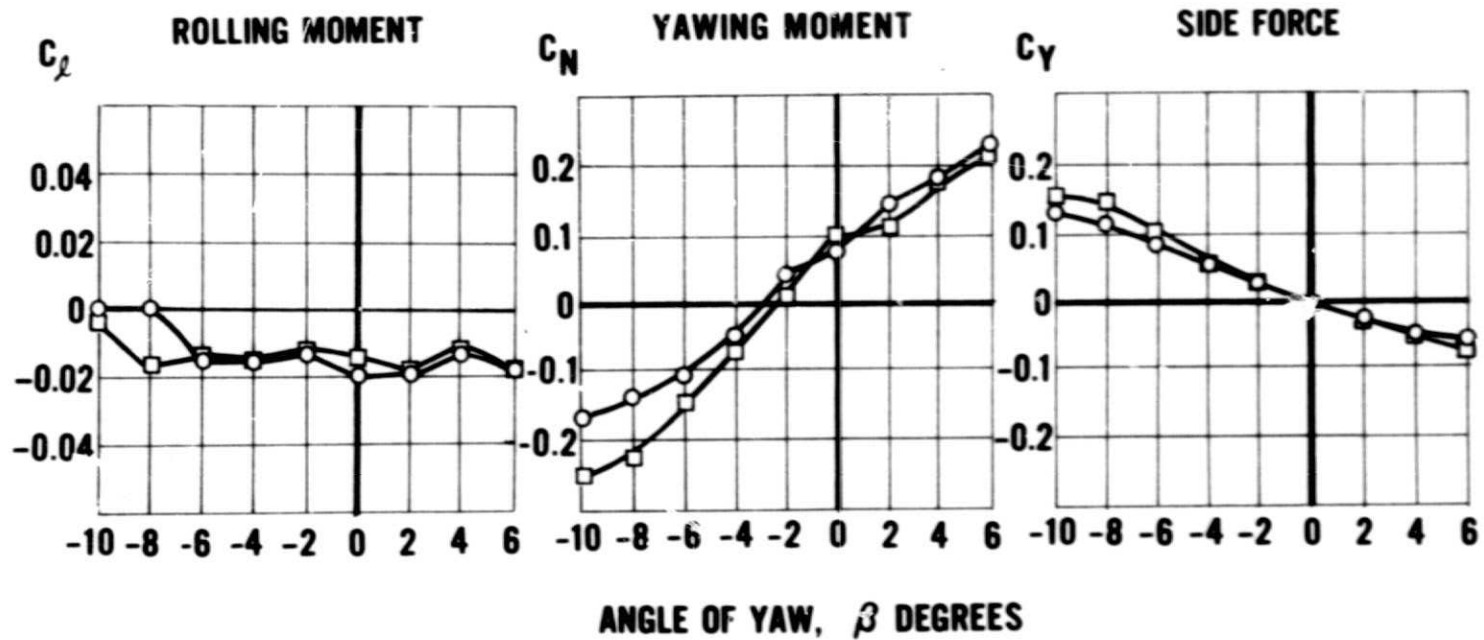


Figure 21.- Longitudinal Trim and Stability Research Aircraft Flight Test.

FLAP ANGLE 75°  
BLOWING COEFFICIENT  $C_{J1} = 0.59$

NOZZLE VECTOR 85°  
NOZZLE THRUST 1500 LB ( $C_T = 0.82$ )



CONVERSION: 0.454 LB = KILOGRAMS

Figure 22.- Lateral Stability. Wind Tunnel Model Tests.

## LANDING FLAP - 65°

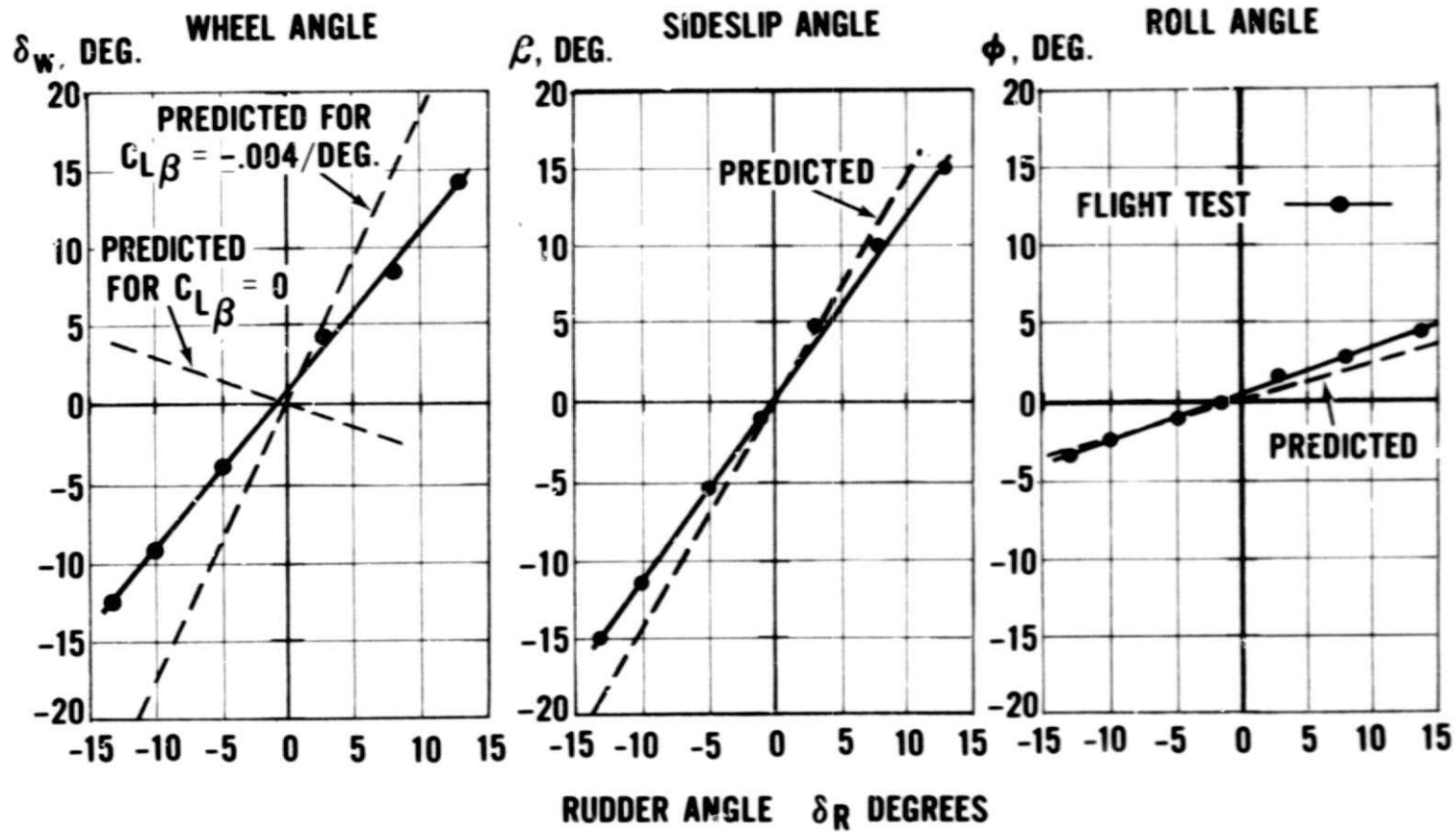
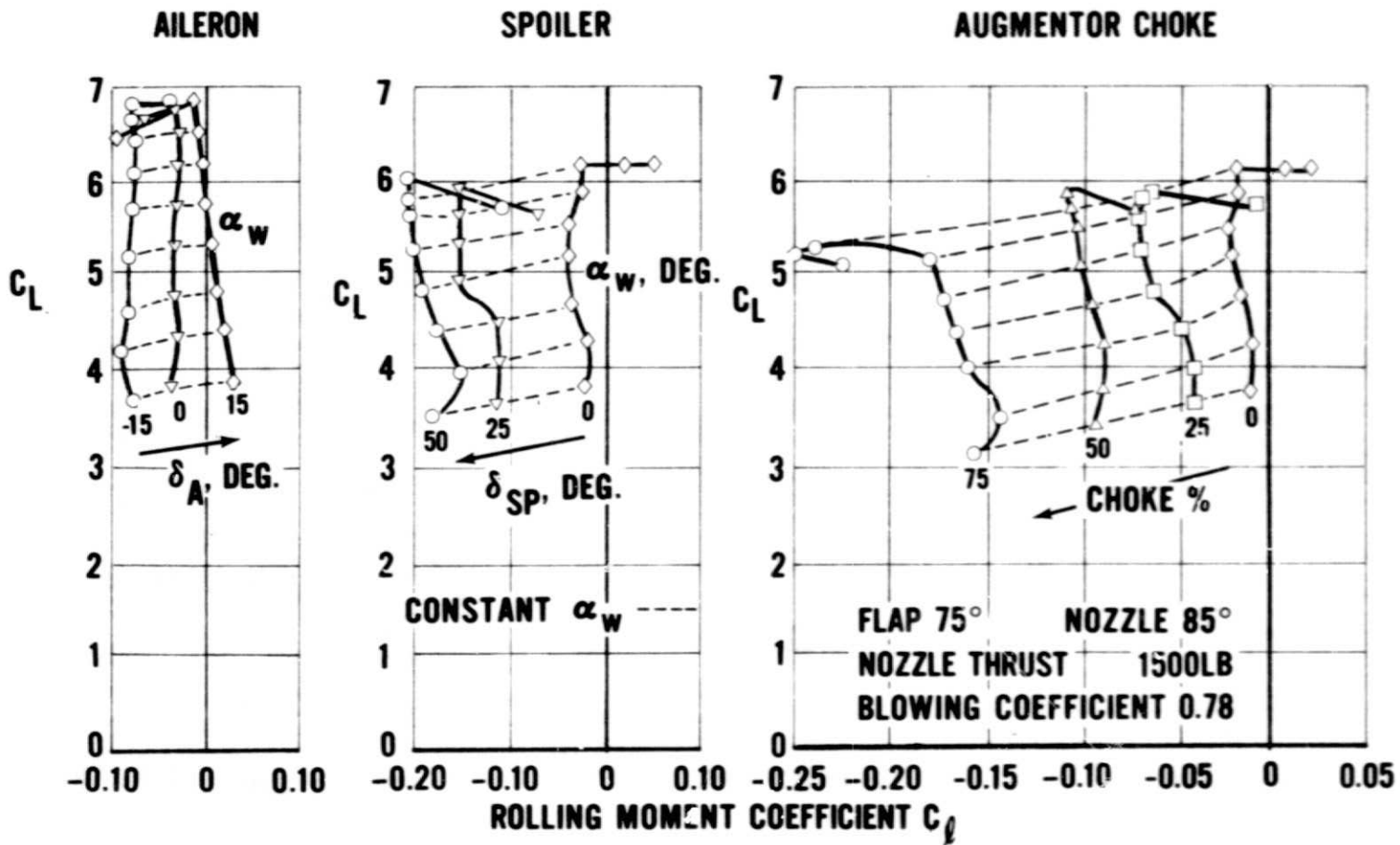


Figure 23.- Lateral Stability. Research Aircraft Flight Tests.



**CONVERSION: 0.454 LB = KILOGRAMS**

Figure 24.- Roll Control Power. Various Controls for Wind Tunnel Model Tests.

FLAP ANGLE 67°  
VELOCITY 69 KT

NOZZLE ANGLE 15°

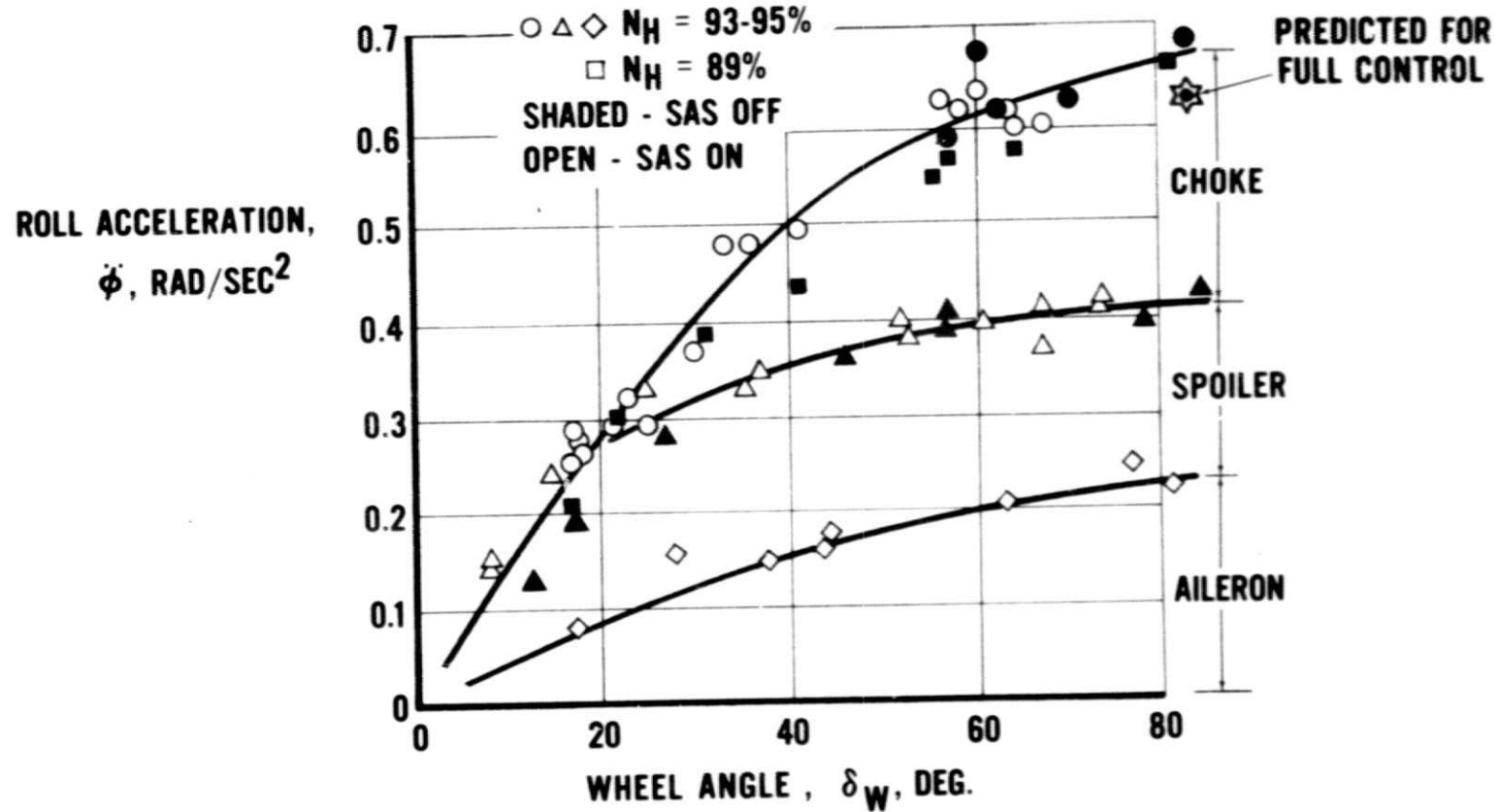


Figure 25.- Roll Control Power. Research Aircraft Flight Tests.